Keep Up with Trends in RF Filtering Techniques p16

How Accurate Models Can Improve Workflows p26

Grating Lobes Take Center Stage in the Phased-Array Antenna Pattern Series p32

Microwaves & RF®

YOUR TRUSTED ENGINEERING RESOURCE FOR OVER 50 YEARS

NOVEMBER 2020 mwrf.com

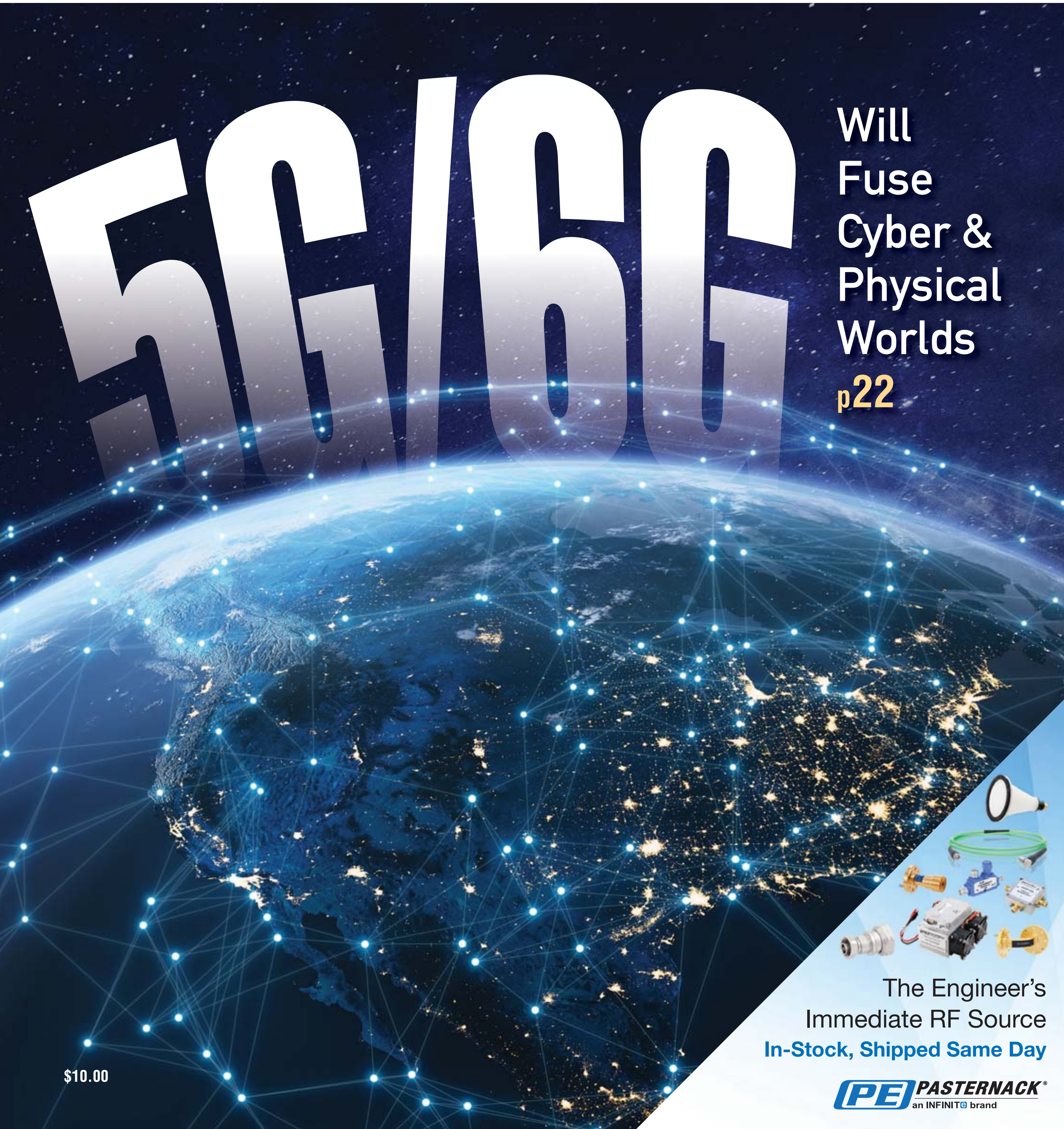

5G/6G Will Fuse Cyber & Physical Worlds

p22

$10.00

cadence®

Design Smarter with AWR Software

See for yourself how easy and effective it is to streamline your design process, improve end-product performance, and accelerate time to market for MMICs, RFICs, RF PCBs, microwave modules, antennas, communications systems, radar systems, and more.

Get started at **cadence.com/go/awr/try**.

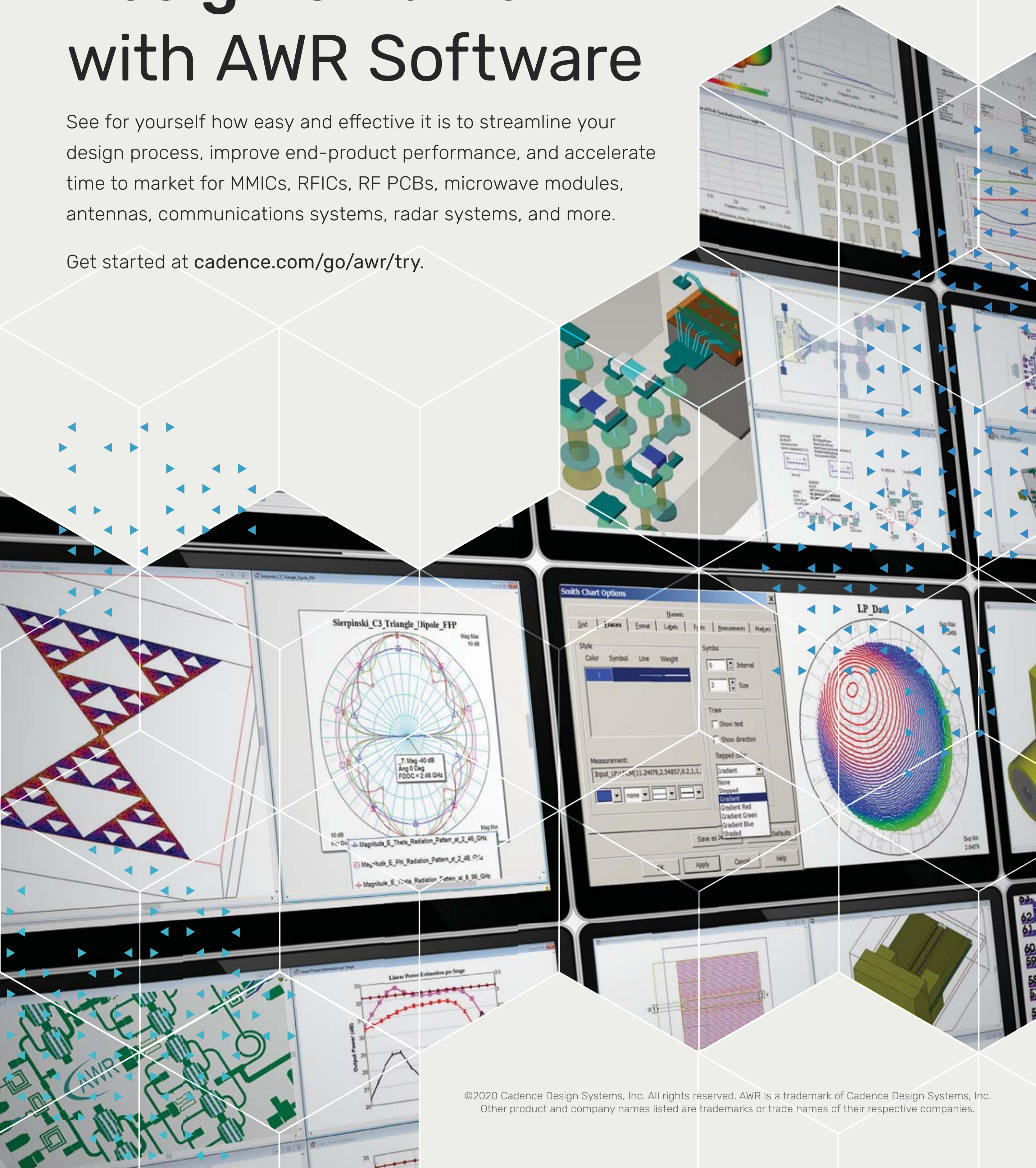

IN THIS ISSUE

FEATURES

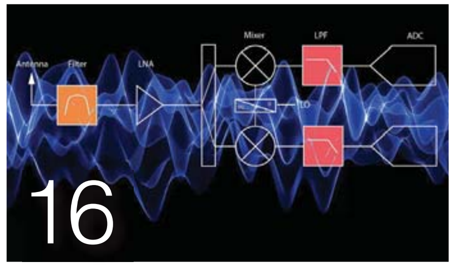

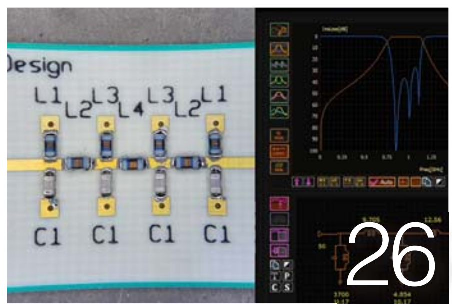

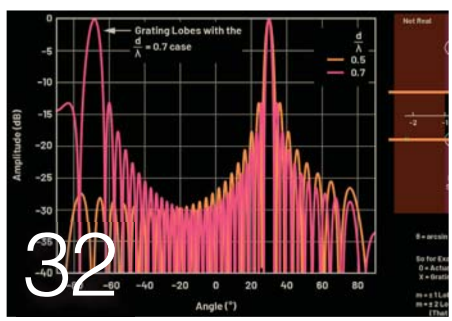

NEWS & COLUMNS

37

JOIN US ONLINE

follow us @MicrowavesRF

become a fan at facebook.com/microwavesRF

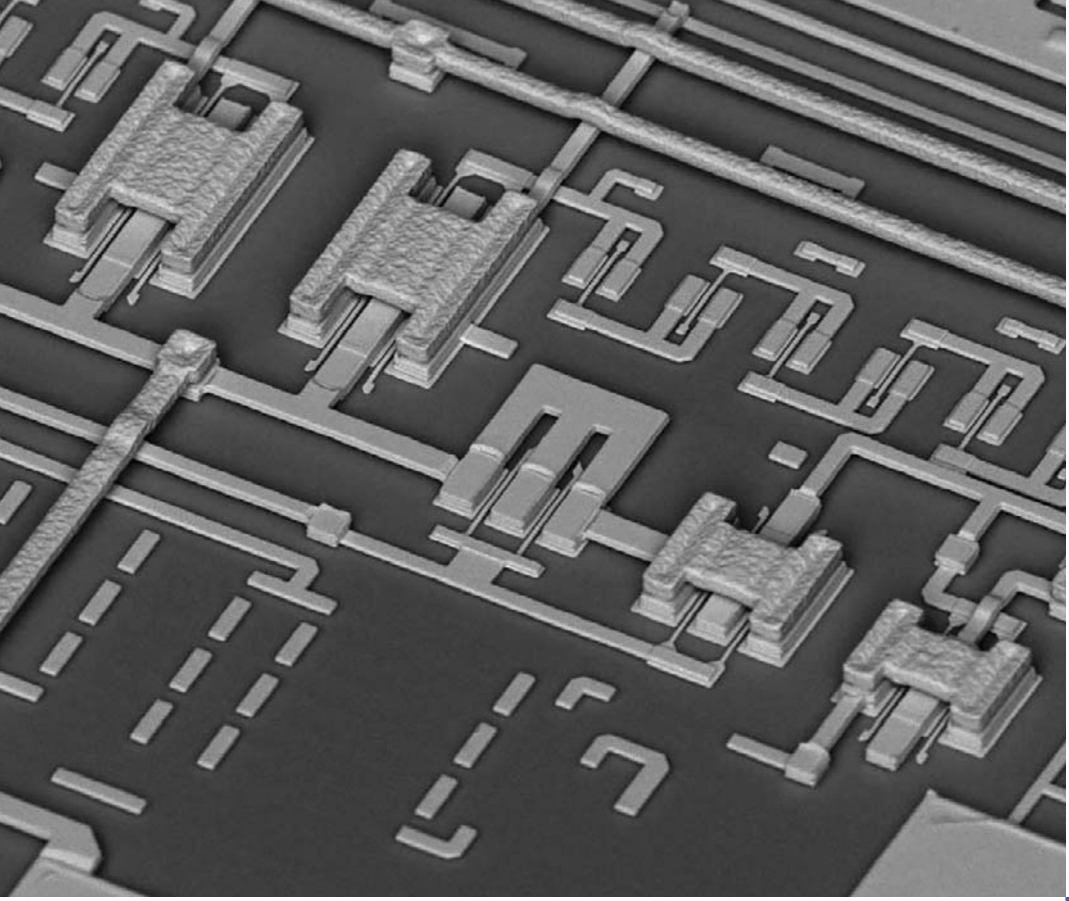

DC TO 50 GHZ

MMIC Products

Wideband

- In-house design expertise and packaging facilities
- 700+ models in stock and growing
- Industry-leading quality and reliability
- All models available in QFN or bare die format

Mini-Circuits®

Editorial
DAVID MALINIAK | Editor
dmaliniak@endeavorb2b.com

5G Phones Arrive, But Has the Network?

You can buy a 5G phone right now. However, can you get real 5G performance? Maybe… or maybe not.

Everybody loves new gadgets, especially those of us with a geeky, techy predisposition (and because you're reading this, I'll naturally assume that includes you). We've been hearing for years already about the new generation of wireless technology that's going to change all our lives for the better. This publication, along with many others, has done more than its share of oohing and aahing over what 5G can and hopefully will do (see this issue's cover story, for example). And it's not all hype either—we believe in the dream and the microwave/RF engineering community's resolve to make it happen.

Tantalizingly, some real, live 5G-capable handsets have arrived in the form of devices like Apple's iPhone 12/12 Pro, Samsung's various Galaxy products, the OnePlus 8 Pro, and Google's Pixel 5. Now, my current smartphone is a couple of years (and product generations) old. It still looks and works like new, the battery is in good shape, and it shows no sign of failing me or even slowing down anytime soon.

So, with a new generation of technology in the offing and begging to be stuffed in my pocket, I begin pondering the notion "should I, or shouldn't I?" What can one expect from a shiny new 5G phone? Can it really teleport me onto the U.S.S. Enterprise like Captain Picard? Or, will I end up wondering why I was in such a hurry to hand over as much as $1,999 for the 5G version of Samsung's Galaxy Z Fold 2?

Well, it depends. The major U.S. carriers (AT&T, T-Mobile, and Verizon) all tout nationwide 5G coverage. But as we all know, their networks are still in the process of being built out. And, in most of that "nationwide coverage," what we're talking about is the low-band flavor of 5G, which isn't much better than 4G LTE—maybe 20% faster data rates. While the carriers attempt to mollify you with that sort of coverage, they continue to proliferate mid-band 5G in large markets. That's a little more like it, but it's certainly not the life-changing experience we've been promised.

Now, millimeter-wave 5G? THAT's a life-changing experience. But to have it, you must bring your 5G phone to a city like New York, Chicago, or San Francisco. And then, you'll have to stand on just the right street corner to find that signal. Verizon, the current leader of the pack, has what it's calling 5G Ultra Wideband fired up in 55 markets across the country. It's probably not coming to my neighborhood anytime soon, and perhaps not yours either.

What it boils down to is this: 5G is very new; it's a costly and lengthy process for the carriers to get their networks up and running in a given area; and, let's face it, it's still somewhat of a product of marketing. That doesn't mean it won't eventually give more of us a chance at that life-changing experience. But it's a matter of time and maturation. Me, I think I'll hang onto my good old LTE banger for now and wait until things mature just a bit more. mw

Microwaves&RF **NOVEMBER 2020**

EDITORIAL

SENIOR CONTENT DIRECTOR: **BILL WONG** bwong@endeavorb2b.com
EDITOR: **DAVID MALINIAK** dmaliniak@endeavorb2b.com
ASSOCIATE EDITOR/COMMUNITY MANAGER: **ROGER ENGELKE** rengelke@endeavorb2b.com
SENIOR STAFF WRITER: **JAMES MORRA** jmorra@endeavorb2b.com
TECHNICAL EDITOR: **JACK BROWNE** jack.browne@citadeleng.com

ART DEPARTMENT

GROUP DESIGN DIRECTOR: **ANTHONY VITOLO** tvitolo@endeavorb2b.com
ART DIRECTOR: **JOCELYN HARTZOG** jhartzog@endeavorb2b.com

PRODUCTION

GROUP PRODUCTION MANAGER: **GREG ARAUJO** garaujo@endeavorb2b.com
PRODUCTION MANAGER: **DEANNA O'BYRNE** dobyrne@endeavorb2b.com

AUDIENCE MARKETING

USER MARKETING MANAGER: **DEBBIE BRADY** dmbrady@endeavorb2b.com
FREE SUBSCRIPTION / STATUS OF SUBSCRIPTION / ADDRESS CHANGE/ MISSING BACK ISSUES:
OMEDA **T** | 847.513.6022 **TOLL FREE** | 866.505.7173 **FAX** | 847.291.4816 microwaves&rf@omeda.com

SALES & MARKETING

REGIONAL SALES REPRESENTATIVES:
AZ, NM, TX: **GREGORY MONTGOMERY** gmontgomery@endeavorb2b.com
AK, NORTHERN CA, NV, OR, WA, WESTERN CANADA: **STUART BOWEN** sbowen@endeavorb2b.com
AL, AR, SOUTHERN CA, CO, FL, GA, HI, IA, ID, IL, IN, KS, KY, LA, MI, MN, MO, MS, MT, NC, ND, NE, OH, OK, SC, SD, TN, UT, VA, WI, WV, WY, CENTRAL CANADA: **JAMIE ALLEN** jallen@endeavorb2b.com
CT, DE, MA, MD, ME, NH, NJ, NY, PA, RI, VT, EASTERN CANADA: **ELIZABETH ELDRIDGE** eeldridge@endeavorb2b.com

INTERNATIONAL SALES:
GERMANY, AUSTRIA, SWITZERLAND: **CHRISTIAN HOELSCHER** christian.hoelscher@highcliffemedia.com
BELGIUM, NETHERLANDS, LUXEMBURG, UNITED KINGDOM, SCANDINAVIA, FRANCE, SPAIN, PORTUGAL:
LARA PHELPS lara.phelps@highcliffemedia.com
ITALY: **DIEGO CASIRAGHI** diego@casiraghi-adv.com
PAN-ASIA: **HELEN LAI** helen@twoway-com.com
PAN-ASIA: **CHARLES LIU** liu@twoway-com.com

REPRINTS: reprints@endeavorb2b.com
LIST RENTALS/ SMARTREACH CLIENT SERVICES MANAGER: **MARY RALICKI** mralicki@endeavorb2b.com

DIGITAL

SENIOR DIGITAL INNOVATION & STRATEGY DIRECTOR: **RYAN MALEC** rmalec@endeavorb2b.com

DESIGN & ENGINEERING GROUP

EVP, DESIGN & ENGINEERING GROUP: **TRACY SMITH** tsmith@endeavorb2b.com
GROUP CONTENT DIRECTOR: **MICHELLE KOPIER** mkopier@endeavorb2b.com
VICE PRESIDENT OF MARKETING SOLUTIONS: **JACQUIE NIEMIEC** jniemiec@endeavorb2b.com

ENDEAVOR BUSINESS MEDIA, LLC

331 54th Ave N., Nashville, TN 37209 USA | www.endeavorbusinessmedia.com
CEO: **CHRIS FERRELL**
CRO/CMO: **JUNE GRIFFIN**
CFO: **WILLIAM NURTHEN**
COO: **PATRICK RAINS**
CHIEF ADMINISTRATIVE AND LEGAL OFFICER: **TRACY KANE**
EVP KEY ACCOUNTS: **SCOTT BIEDA**
EVP SPECIAL PROJECTS: **KRISTINE RUSSELL**

ENDEAVOR BUSINESS MEDIA

Electronic Design | Machine Design | Microwaves & RF | Hydraulics & Pneumatics | Source ESB | Source Today | Evaluation Engineering

ON MICROWAVES&RF.COM

Magnetic-Field Navigation as an "Alternative" GPS?

By using measurements of anomalies in the Earth's magnetic field and machine learning to extract data from raw signals, then matching them to accurate magnetic-anomaly maps, it may be possible to navigate aircraft with reasonable accuracy independent of GPS.

https://www.mwrf.com/technologies/systems/article/21145895/magneticfield-navigation-as-an-alternative-gps

11 Myths About Cellular IoT Design

Laird Connectivity's Jonathan Kaye discusses the most common misconceptions about cellular IoT design—a growing area of IoT thanks to two new versions of the cellular standard that enable battery life of up to 10 years for wireless devices.

https://www.mwrf.com/technologies/systems/article/21140965/11-myths-about-cellular-iot-design

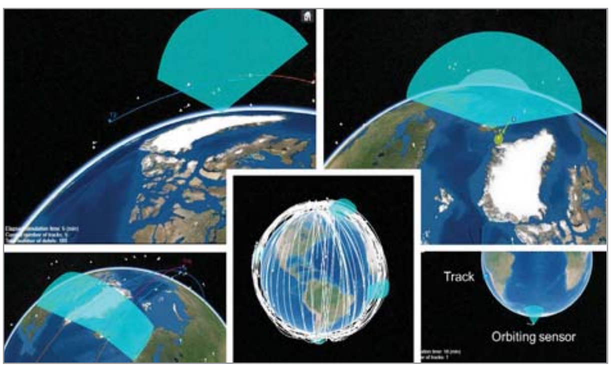

Tracking Space Debris with a Radar Network

This "Algorithms to Antenna" installment shows how to model a network of radar systems that looks into space with a goal of tracking debris orbiting Earth.

https://www.mwrf.com/technologies/systems/article/21145361/algorithms-to-antenna-tracking-space-debris-with-a-radar-network

Rent, Lease, or Buy Electronic Test Equipment? Here's How to Decide

Evolving technology, certifications, and time are just some of the points to consider before renting, leasing, or buying that next piece of equipment.

https://www.mwrf.com/technologies/test-measurement/article/21141292/rent-lease-or-buy-electronic-test-equipment-heres-how-to-decide

join us online

twitter.com/MicrowavesRF facebook.com/microwavesrf

RF Amplifiers and Sub-Assemblies for Every Application

Delivery from Stock to 2 Weeks ARO from the catalog or built to your specifications!

- Competitive Pricing & Fast Delivery
- Military Reliability & Qualification
- Various Options: Temperature Compensation, Input Limiter Protection, Detectors/TTL & More
- Unconditionally Stable (100% tested)

ISO 9001:2000 and AS9100B CERTIFIED

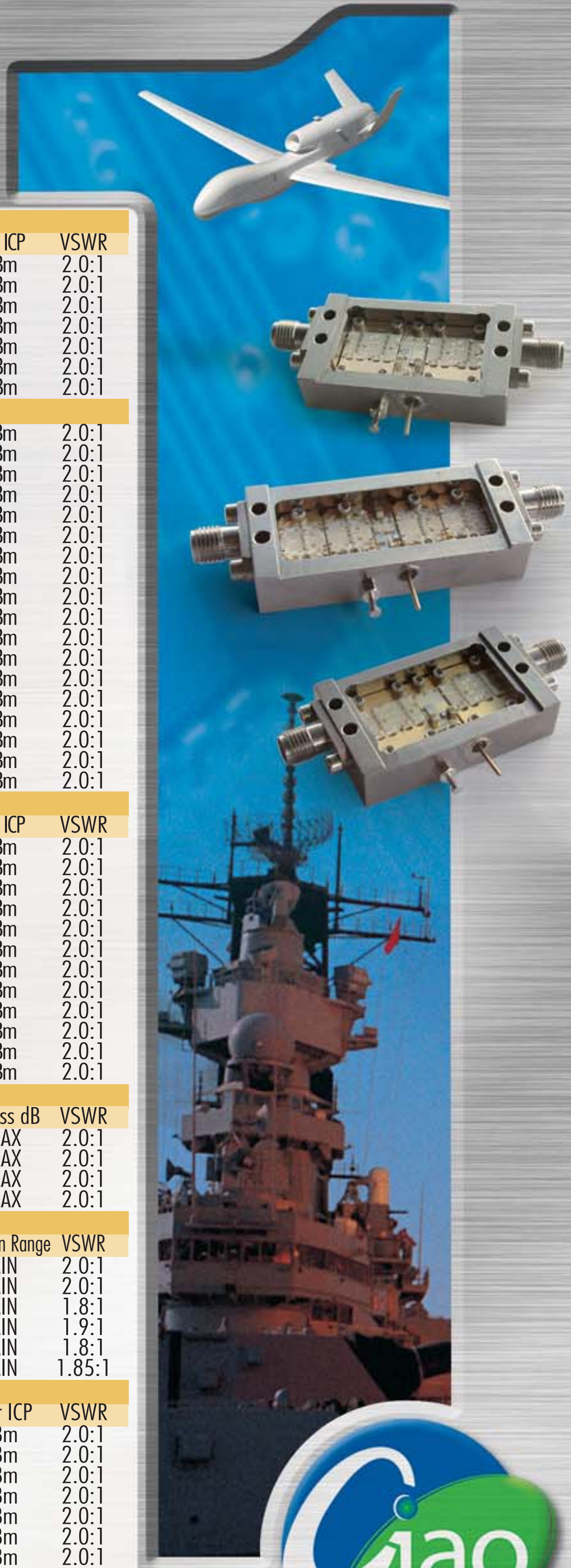

OCTAVE BAND LOW NOISE AMPLIFIERS

Model No.	Freq (GHz)	Gain (dB) MIN	Noise Figure (dB)	Power-out @ P1-dB	3rd Order ICP	VSWR
CA01-2110	0.5-1.0	28	1.0 MAX, 0.7 TYP	+10 MIN	+20 dBm	2.0:1
CA12-2110	1.0-2.0	30	1.0 MAX, 0.7 TYP	+10 MIN	+20 dBm	2.0:1
CA24-2111	2.0-4.0	29	1.1 MAX, 0.95 TYP	+10 MIN	+20 dBm	2.0:1
CA48-2111	4.0-8.0	29	1.3 MAX, 1.0 TYP	+10 MIN	+20 dBm	2.0:1
CA812-3111	8.0-12.0	27	1.6 MAX, 1.4 TYP	+10 MIN	+20 dBm	2.0:1
CA1218-4111	12.0-18.0	25	1.9 MAX, 1.7 TYP	+10 MIN	+20 dBm	2.0:1
CA1826-2110	18.0-26.5	32	3.0 MAX, 2.5 TYP	+10 MIN	+20 dBm	2.0:1

NARROW BAND LOW NOISE AND MEDIUM POWER AMPLIFIERS

Model No.	Freq (GHz)	Gain (dB) MIN	Noise Figure (dB)	Power-out @ P1-dB	3rd Order ICP	VSWR
CA01-2111	0.4 - 0.5	28	0.6 MAX, 0.4 TYP	+10 MIN	+20 dBm	2.0:1
CA01-2113	0.8 - 1.0	28	0.6 MAX, 0.4 TYP	+10 MIN	+20 dBm	2.0:1
CA12-3117	1.2 - 1.6	25	0.6 MAX, 0.4 TYP	+10 MIN	+20 dBm	2.0:1
CA23-3111	2.2 - 2.4	30	0.6 MAX, 0.45 TYP	+10 MIN	+20 dBm	2.0:1
CA23-3116	2.7 - 2.9	29	0.7 MAX, 0.5 TYP	+10 MIN	+20 dBm	2.0:1
CA34-2110	3.7 - 4.2	28	1.0 MAX, 0.5 TYP	+10 MIN	+20 dBm	2.0:1
CA56-3110	5.4 - 5.9	40	1.0 MAX, 0.5 TYP	+10 MIN	+20 dBm	2.0:1
CA78-4110	7.25 - 7.75	32	1.2 MAX, 1.0 TYP	+10 MIN	+20 dBm	2.0:1
CA910-3110	9.0 - 10.6	25	1.4 MAX, 1.2 TYP	+10 MIN	+20 dBm	2.0:1
CA1315-3110	13.75 - 15.4	25	1.6 MAX, 1.4 TYP	+10 MIN	+20 dBm	2.0:1
CA12-3114	1.35 - 1.85	30	4.0 MAX, 3.0 TYP	+33 MIN	+41 dBm	2.0:1
CA34-6116	3.1 - 3.5	40	4.5 MAX, 3.5 TYP	+35 MIN	+43 dBm	2.0:1
CA56-5114	5.9 - 6.4	30	5.0 MAX, 4.0 TYP	+30 MIN	+40 dBm	2.0:1
CA812-6115	8.0 - 12.0	30	4.5 MAX, 3.5 TYP	+30 MIN	+40 dBm	2.0:1
CA812-6116	8.0 - 12.0	30	5.0 MAX, 4.0 TYP	+33 MIN	+41 dBm	2.0:1
CA1213-7110	12.2 - 13.25	28	6.0 MAX, 5.5 TYP	+33 MIN	+42 dBm	2.0:1
CA1415-7110	14.0 - 15.0	30	5.0 MAX, 4.0 TYP	+30 MIN	+40 dBm	2.0:1
CA1722-4110	17.0 - 22.0	25	3.5 MAX, 2.8 TYP	+21 MIN	+31 dBm	2.0:1

ULTRA-BROADBAND & MULTI-OCTAVE BAND AMPLIFIERS

Model No.	Freq (GHz)	Gain (dB) MIN	Noise Figure (dB)	Power-out @ P1-dB	3rd Order ICP	VSWR
CA0102-3111	0.1-2.0	28	1.6 Max, 1.2 TYP	+10 MIN	+20 dBm	2.0:1
CA0106-3111	0.1-6.0	28	1.9 Max, 1.5 TYP	+10 MIN	+20 dBm	2.0:1
CA0108-3110	0.1-8.0	26	2.2 Max, 1.8 TYP	+10 MIN	+20 dBm	2.0:1
CA0108-4112	0.1-8.0	32	3.0 MAX, 1.8 TYP	+22 MIN	+32 dBm	2.0:1
CA02-3112	0.5-2.0	36	4.5 MAX, 2.5 TYP	+30 MIN	+40 dBm	2.0:1
CA26-3110	2.0-6.0	26	2.0 MAX, 1.5 TYP	+10 MIN	+20 dBm	2.0:1
CA26-4114	2.0-6.0	22	5.0 MAX, 3.5 TYP	+30 MIN	+40 dBm	2.0:1
CA618-4112	6.0-18.0	25	5.0 MAX, 3.5 TYP	+23 MIN	+33 dBm	2.0:1
CA618-6114	6.0-18.0	35	5.0 MAX, 3.5 TYP	+30 MIN	+40 dBm	2.0:1
CA218-4116	2.0-18.0	30	3.5 MAX, 2.8 TYP	+10 MIN	+20 dBm	2.0:1
CA218-4110	2.0-18.0	30	5.0 MAX, 3.5 TYP	+20 MIN	+30 dBm	2.0:1
CA218-4112	2.0-18.0	29	5.0 MAX, 3.5 TYP	+24 MIN	+34 dBm	2.0:1

LIMITING AMPLIFIERS

Model No.	Freq (GHz)	Input Dynamic Range	Output Power Range Psat	Power Flatness dB	VSWR
CLA24-4001	2.0 - 4.0	-28 to +10 dBm	+7 to +11 dBm	+/- 1.5 MAX	2.0:1
CLA26-8001	2.0 - 6.0	-50 to +20 dBm	+14 to +18 dBm	+/- 1.5 MAX	2.0:1
CLA712-5001	7.0 - 12.4	-21 to +10 dBm	+14 to +19 dBm	+/- 1.5 MAX	2.0:1
CLA618-1201	6.0 - 18.0	-50 to +20 dBm	+14 to +19 dBm	+/- 1.5 MAX	2.0:1

AMPLIFIERS WITH INTEGRATED GAIN ATTENUATION

Model No.	Freq (GHz)	Gain (dB) MIN	Noise Figure (dB)	Power-out @ P1-dB	Gain Attenuation Range	VSWR
CA001-2511A	0.025-0.150	21	5.0 MAX, 3.5 TYP	+12 MIN	30 dB MIN	2.0:1
CA05-3110A	0.5-5.5	23	2.5 MAX, 1.5 TYP	+18 MIN	20 dB MIN	2.0:1
CA56-3110A	5.85-6.425	28	2.5 MAX, 1.5 TYP	+16 MIN	22 dB MIN	1.8:1
CA612-4110A	6.0-12.0	24	2.5 MAX, 1.5 TYP	+12 MIN	15 dB MIN	1.9:1
CA1315-4110A	13.75-15.4	25	2.2 MAX, 1.6 TYP	+16 MIN	20 dB MIN	1.8:1
CA1518-4110A	15.0-18.0	30	3.0 MAX, 2.0 TYP	+18 MIN	20 dB MIN	1.85:1

LOW FREQUENCY AMPLIFIERS

Model No.	Freq (GHz)	Gain (dB) MIN	Noise Figure dB	Power-out @ P1-dB	3rd Order ICP	VSWR
CA001-2110	0.01-0.10	18	4.0 MAX, 2.2 TYP	+10 MIN	+20 dBm	2.0:1
CA001-2211	0.04-0.15	24	3.5 MAX, 2.2 TYP	+13 MIN	+23 dBm	2.0:1
CA001-2215	0.04-0.15	23	4.0 MAX, 2.2 TYP	+23 MIN	+33 dBm	2.0:1
CA001-3113	0.01-1.0	28	4.0 MAX, 2.8 TYP	+17 MIN	+27 dBm	2.0:1
CA002-3114	0.01-2.0	27	4.0 MAX, 2.8 TYP	+20 MIN	+30 dBm	2.0:1
CA003-3116	0.01-3.0	18	4.0 MAX, 2.8 TYP	+25 MIN	+35 dBm	2.0:1
CA004-3112	0.01-4.0	32	4.0 MAX, 2.8 TYP	+15 MIN	+25 dBm	2.0:1

CIAO Wireless can easily modify any of its standard models to meet your "exact" requirements at the Catalog Pricing.

Visit our web site at **www.ciaowireless.com** for our complete product offering.

Ciao wireless

Ciao Wireless, Inc. 4000 Via Pescador, Camarillo, CA 93012

Tel (805) 389-3224 Fax (805) 389-3629 sales@ciaowireless.com

News

Tiny Bluetooth Modules Run 10 Years on SINGLE-CELL BATTERY

Powered by a CR2354 battery, this minuscule Bluetooth SoC can be a standalone wireless solution or a wireless support device.

Silicon Labs' BGM220 system-on-chip (SoC) packs a pair of Arm cores to manage Bluetooth communication that spans the standards from Bluetooth 4.x through 5.2 as well as Bluetooth mesh *(Fig. 1)*. It can operate for a decade using just a single-cell CR2354 battery, providing Bluetooth communication over that span.

A dedicated Cortex-M0+ handles real-time chores and the radios, while a Cortex-M33 runs the bulk of the Bluetooth stack with plenty of headroom for applications *(Fig. 2 on page 10)*. Thanks to the modular software configuration, developers can choose which standards to utilize to optimize power, range, and throughput for their application.

The 4- × 4-mm, QFN32 BGM220 chip is available separately or incorporated into two compact system-in-package (SiP) solutions. The 6- × 6-mm BGM220S adds an on-board antenna and an RF pin coupled to a +6-dBm transmitter. Both SiPs incorporate up to 25 GPIOs; the full GPIO complement requires a 5- × 5-mm QFN40 package.

The larger BGM220P is built on a 13- × 15-mm PCB and the transmitter can operate up to +8 dBm. It also has a built-in antenna and can be used with or without a built-in LFXO. The BGM220P provides more range at a low cost.

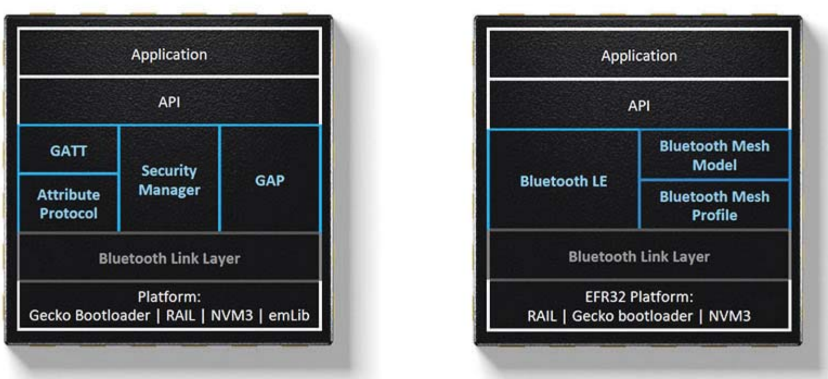

1. Developers can choose from a compact Bluetooth LE stack (left) or add mesh-networking support (right).

The SiPs integrate dc-dc power management plus all passives and on-board crystals. Versions are available that can handle extended temperatures up to 105°C. They're Bluetooth 5.2 certified and address standards such as CE, FCC/ISED, MIC, and Telec.

The BGM220 has up to 512 kB of flash memory shared by both processors. There's also up to 32 kB of RAM. Active current is 25 µA/MHz while the full 32 kB of RAM can be maintained in sleep mode for 1.4 µA. Operating voltage range is 1.71 to 3.8 V.

The radios support Bluetooth 5.2 and Bluetooth mesh LPN (low power node) as well as 1M, 2M, Bluetooth Low Energy (BLE) Coded PHY audio, and angle of arrival (AoA)/departure (AoD) for location support. Proprietary 2.4-GHz support can handle 2/4(G)FSK, (G)MSK, OQPSK, and DSSS.

Silicon Labs provides development tools in addition to the configurable protocol stacks. The Xpress option offers a pre-programmed API-driven solution that allows developers to concentrate on their application while taking advantage of wireless connectivity.

Developers can use Silicon Labs' Simplicity Studio to tune their Bluetooth stack, depending on the features they

DC TO 86 GHZ

Filter Solutions

For Every Application

Selection and Solutions

- 300+ in-stock models
- Low pass, high pass, band pass, diplexers and triplexers
- Cost-effective custom designs with fast turnaround

Technologies:

LTCC, lumped L-C, ceramic resonator, reflectionless filters, suspended substrate, microstrip, alumina, cavity, waveguide

Mini-Circuits®

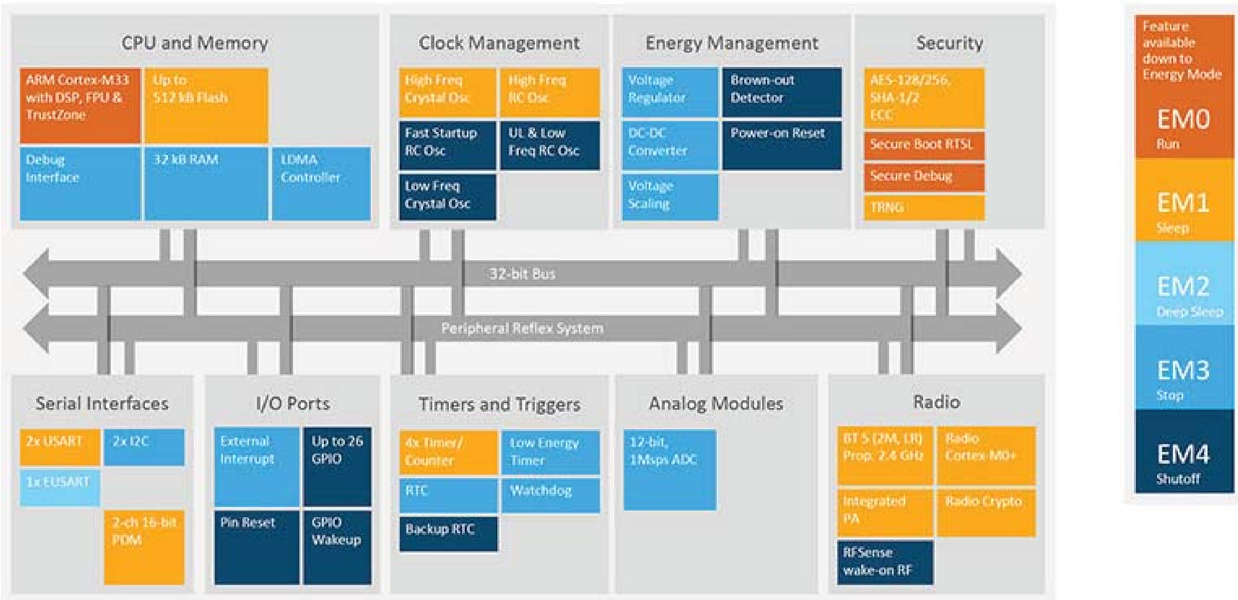

2. The BGM220 includes a Cortex-M0+ for real-time radio control and a Cortex-M33 application processor.

need. For example, BLE requires only 158 kB of flash while a full-blown mesh stack runs about 300 kB. There's also a stripped-down mesh node configuration. This enables the chip to handle chores from a high-end gateway to very low power nodes.

The company also built in Wi-Fi Packet Traffic Arbitration (PTA) coexistence support. This four-wire interface allows a host processor to manage the Bluetooth transmitters with its other wireless transmitters so that they don't try to use the same bands at the same time. Essentially, the interface includes request to transmit, allow transmission, and a priority line.

The chip is designed for secure solutions starting with a root of trust and secure loader (RTSL). This includes secure boot support as well as secure, over-the-air updates.

Silicon Labs provides a range of evaluation and development platforms *(Fig. 3)*, starting with a low-end node to a complete platform with interchangeable radios.

The BGM220 can act as a standalone wireless solution as well as become a wireless support device for a host. The latter is often a gateway platform, such as a Wi-Fi device that may be a Bluetooth bridge, or use Bluetooth for local wireless configuration and management. ■

The chip is designed for secure solutions starting with a root of trust and secure loader (RTSL). This includes secure boot support as well as secure, over-the-air updates.

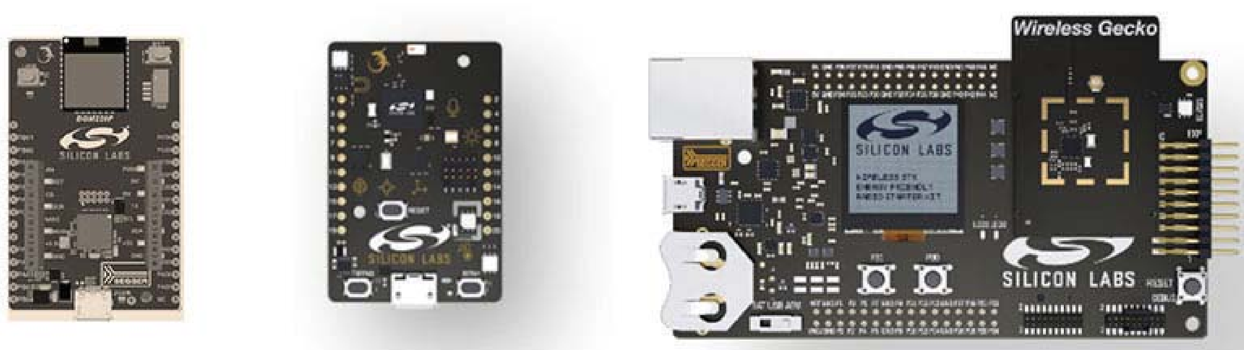

3. The Explorer kit (left) is priced under $10, while the more functional SLTB010A development kit (center) costs less than $40. The Pro Development Kit (right) supports multiprotocol development and interchangeable radio cards.

LAB-BASED "Li-Fi" LINK Exceeds 7 Gb/s Using Blue Micro LED

AS AN OPTICALLY BASED COMPLEMENT to RF-based Wi-Fi, Li-Fi (light fidelity) offers distinct attributes including potentially extremely high throughout over limited distances and immunity from (and non-sourcing of) EMI/RFI. One other characteristic of an optical link can be considered either a benefit or a drawback: Its line-of-sight path provides outstanding immunity to eavesdropping and hacking, but also limits user mobility.

Adoption of Li-Fi in the marketplace has been very limited thus far. However, there's an industry association that provides standards and support, and there's the potential for using a single LED bulb/photoreceptor unit as both light source and Li-Fi node *(see Resources).*

Researchers, of course, see pushing the envelope of optical-based data links as an area of great interest. A team at Leti (a research institute of CEA Tech, Grenoble, France) has achieved a visible light communication (VLC) test-bed transmission at 7.7 Gb/s (significantly exceeding the previous 5.1-Gb/s record) using a single, 10-µm diameter, gallium-nitride (GaN) blue micro LED *(Fig. 1)*. (In general, a smaller emissive area of the LED yields a higher bandwidth—here, 1.8 GHz in the institute's single-blue micro LED project.)

In addition to the micro LED, the team also developed an advanced multi-carrier modulation scheme combined with digital signal processing to achieve their results. This high spectrum-efficiency waveform was transmitted by the single LED, received on a high-speed photodetector, and demodulated using a direct sampling oscilloscope *(Fig. 2 on page 12).*

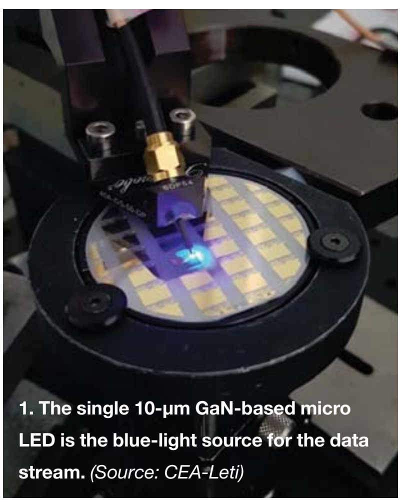

1. The single 10-µm GaN-based micro LED is the blue-light source for the data stream. *(Source: CEA-Leti)*

This class of experimental test bed requires many electro-optical components as well as test-and-measurement equipment for support, including these:

- Keithley (Tektronix) 2601 Current/voltage Source /DC Supply

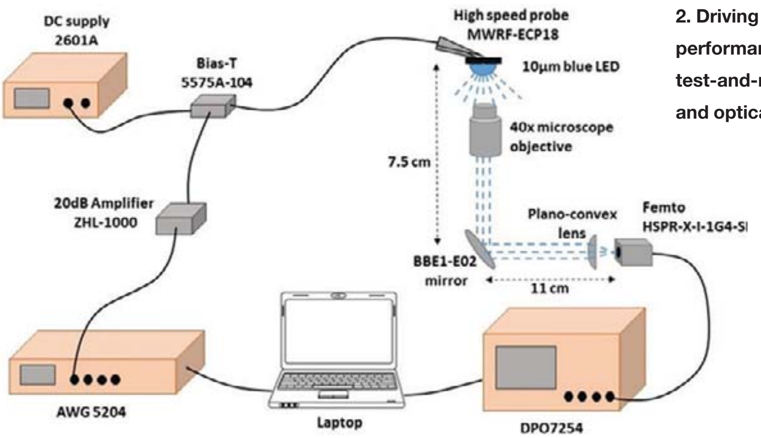

2. Driving the micro LED, creating the link, and assessing its performance takes a significant amount of high-performance test-and-measurement equipment along with electro-optics and optical components. *(Source: CEA-Leti)*

- Mini-Circuits ZHL-1000-3W 3W, 500 to 1000 MHz Amplifier
- Tektronix AWG5204 Arbitrary Waveform Generator
- Microworld MWRF-ECP18 18-GHz RF probe
- Femto HSPR-X2 GHz Ultra-Fast Photoreceiver
- Thor Labs BBE1-E02 - 1" Broadband Dielectric Elliptical Mirror
- Tektronix 7254 Digital Oscilloscope
- Picosecond Pulse Labs (Tektronix) 5575A Bias Tee

While the Light Communications Alliance (created in 2019) is intended to encourage the industry to implement standardization and promote interoperability between Li-Fi systems from different manufacturers, CEA-Leti is planning to continue its research in two areas:

- Developing a better understanding of the electrical behavior of single LEDs in high-frequency regimes and the link between bandwidth and electromigration patterns.
- Investigating techniques to improve the range and/or increase the data rate using a matrix of multi-LED emissive devices. This requires adapting the waveform generation as well as a CMOS interposer to drive the matrix on a pixel basis.

LiFi RESOURCES

- http://lightcommunications.org/
- https://standards.ieee.org/standard/802_15_7-2018.html
- https://www.lifitn.com/im-new
- https://en.wikipedia.org/wiki/Li-Fi#Standards

Planar Monolithics Industries, Inc.

mmWave Limiters up to 50 GHz

PMI offers a variety of mmWave Limiters capable of withstanding an input power level of 20 Watts for military and industrial applications. PMI's limiters offer low loss, fast recovery along with low RF leakage levels and broadband coverage to 50 GHz. More available at: https://www.pmi-rf.com/categories/limiters

2-IN-1 - Dual Use Connectorized or Surface Mount


LM-10M35G-15DBM-4W-292FF
LM-10M40G-15DBM-4W-AGAL
LM-10M50G-18DBM-4W-24FF


LM-18G40G-SMT-1


LM-18G40G-18-1W-292FF


LM-26G40G-14-20W-292FF
LM-26G40G-14-20W-292FF Rev. B

PMI Model No.	FREQ Range (GHz)	Insertion Loss (dB)	Input Power (Peak)	Leakage Power (dBm)	Recovery Time	Size (Inches) / Connectors
LM-10M35G-15DBM-4W-292FF https://www.pmi-rf.com/product-details/lm-10m35g-15dbm-4w-292ff	10 MHz - 35	4.0	25 W CW (20 MHz - 18 GHz) & 50 - 40 W PW (20 MHz - 18 GHz), 1 µs PW, 1% duty cycle	+18	150 ns	0.53" X 0.7" X 0.26" 2.92mm (F) Field Removable and SMT (Drop-In)
LM-10M40G-15DBM-4W-AGAL https://www.pmi-rf.com/product-details/lm-10m40g-15dbm-4w-agal	10 MHz - 40	3.2	5 W CW (20 MHz - 12 GHz), 20 W (18 GHz), 1 µs PW, 1% duty cycle	+22	100 ns	0.53" X 0.7" X 0.26" 2.92mm (F) Field Removable and SMT (Drop-In)
LM-10M50G-18DBM-4W-24FF https://www.pmi-rf.com/product-details/lm-10m50g-18dbm-4w-24ff	10 MHz - 50	3.4	4 W CW & 20 W peak, PW 1 µs to 10 µs, 1% duty cycle	+18	100 ns	0.53" X 0.7" X 0.26" 2.92mm (F) Field Removable and SMT (Drop-In)
LM-18G40G-SMT-1 https://www.pmi-rf.com/product-details/lm-18g40g-smt-1	18 - 40	4	20 W peak, 440 - 670 ns PW, PRF 600 - 900 kHz, 40% Duty Cycle	+14	250 ns	0.27" X 0.198" X 0.016" surface mount / drop-in carrier
LM-18G40G-18-1W-292FF https://www.pmi-rf.com/product-details/lm-18g40g-18-1w-292ff-	18 - 40	4	1 W CW	+18	10 ns	0.5" X 0.5" X 0.22" 2.92mm (F/F) Field Removable
LM-26G40G-14-20W-292FF https://www.pmi-rf.com/product-details/lm-26g40g-14-20w-292ff	26.5 - 40	4	20 W peak, 440 - 670 ns PW, PRF 600 - 900 kHz, 40% Duty Cycle	+14	250 ns	0.5" X 0.5" X 0.22" 2.92mm (F/F) Field Removable
LM-26G40G-14-20W-292FF Rev. B https://www.pmi-rf.com/product-details/lm-26g40g-14-20w-292ff-rev-b	26.5 - 40	4	20 W peak, 440 - 670 ns PW, PRF 600 - 900 kHz, 40% Duty Cycle	+14	250 ns	0.5" X 0.5" X 0.22" 2.92mm (F/F) Field Removable
LM-26G40G-14-20W-292FM https://www.pmi-rf.com/product-details/lm-26g40g-14-20w-292fm	26.5 - 40	4	20 W peak, 440 - 670 ns PW, PRF 600 - 900 kHz, 40% Duty Cycle	+14	250 ns	0.5" X 0.5" X 0.22" 2.92mm (F/M) Field Removable
LM-26G40G-14-20W-292MM https://www.pmi-rf.com/product-details/lm-26g40g-14-20w-292mm	26.5 - 40	4	20 W peak, 440 - 670 ns PW, PRF 600 - 900 kHz, 40% Duty Cycle	+14	250 ns	0.5" X 0.5" X 0.22" 2.92mm (M/M) Field Removable
LM-32G36G-14-20W-SMT https://www.pmi-rf.com/product-details/lm-32g36g-14-20w-smt	32 - 36	2	20 W peak, 30 µs PW, 30% Duty Cycle	+14	250 ns	0.53" X 0.7" X 0.26" 2.92mm (F) Field Removable and SMT (Drop-In)
LM-35D5G-14-20W-292FF https://www.pmi-rf.com/product-details/lm-35d5g-14-20w-292ff	35 - 36	3	20 W, 440 - 670 ns PW, PRF 600 - 900 kHz, 40% Duty Cycle	+14	250 ns	0.5" X 0.5" X 0.22" 2.92mm (F/F) Field Removable


LM-26G40G-14-20W-292FM


LM-26G40G-14-20W-292MM


LM-32G36G-14-20W-SMT


LM-35D5G-14-20W-292FF

Amplifiers - Solid State
Attenuators - Variable/ Programmable
Bi-Phase Modulators
Couplers (Quadrature, 180, Directional)
Detectors - RF / Microwave
DLVAs, ERDLVAs & SDLVAs
Filters & Switched Filter Banks
Form, Fit, Functional Products & Services
Frequency Converters
Frequency Sources
Frequency Discriminators & IFM
Frequency Synthesizers
Gain & Loss Equalizers
Integrated MIC/MMIC Assemblies (IMAs)
IQ Vector Modulators
Limiters - RF / Microwave
Log Amps
Miscellaneous Products
Monopulse Comparators
Multifunction Integrated Assemblies (IMAs)
Phase Shifters & Bi-Phase Modulators
Power Dividers/Combiners (Passive & Active)
Pulse Modulators - SPST
Rack & Chassis Mount Products
Receiver Front Ends & Transceivers
Single Side Band Modulators
SMT & QFN Products
Switch Matrices
Switch Filter Banks
Switches - Solid-State
Systems - Radar Sense & Avoid
Systems - Fly Eye Radar
Threshold Detectors
USB Products

West Coast Operation:
4921 Robert J. Mathews Pkwy, Suite 1
El Dorado Hills, CA 95762 USA
Tel: 916-542-1401, Fax: 916-265-2597

East Coast Operation:
7311-F Grove Road
Frederick, MD 21704 USA
Tel: 301-662-5019, Fax: 301-662-1731

sales@pmi-rf.com • www.pmi-rf.com

ISO9001-2015 REGISTERED

DC TO MMWAVE

Preferred by 20,000+

More than Just a Supplier

Selection and Solutions

- 27 Product lines from one source
- 7500+ Models in stock and growing
- Coverage from VHF to mmWave
- Custom components, integrated systems and test solutions with fast turnaround

Service

- Global presence, local service
- Accessible engineering and support
- Same-day shipping and on-time delivery
- Short lead times and low minimums

Peace of Mind

- Award-winning quality excellence
- Easy troubleshooting and RMA process
- Supply chain security through the life of your system – no EOL target

Constant Innovation

- Relentless investment in new products and design capabilities
- 400+ Catalog introductions per year
- Patented technologies

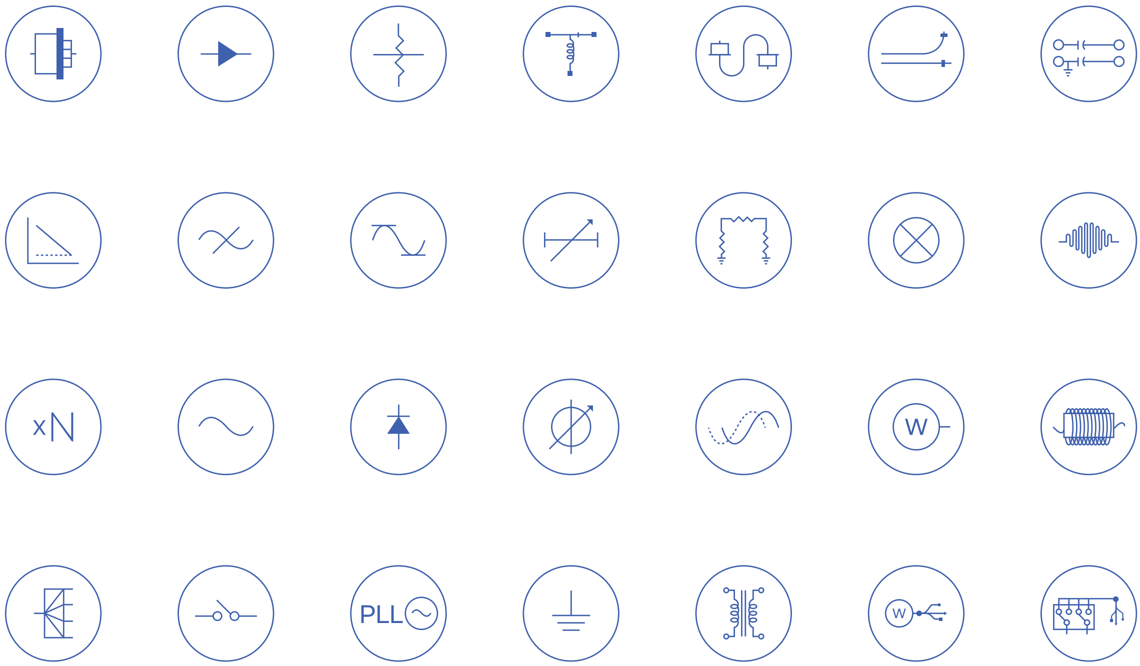

Mini-Circuits®

PETER MATTHEWS | Senior Technical Marketing Manager, Knowles Precision Devices (KPD)

Keep Abreast of RF Filtering Trends (Part 1)

The opener of this two-part series examines the current trends in filter design in the context of the challenges presented by today's highly complex RF environment.

At any given time, a multitude of signals at various frequencies are streaming all around us. Devices such as televisions, radios, radars, medical devices, and cell phones rely on receiving the proper RF signal to deliver what's expected by the end user. Therefore, each of these devices requires some level of filtering to attenuate or remove unwanted signals from the desired channel. Without filtering, these devices can become saturated and unwanted signals can combine with desired signals to corrupt information.

While all filters have the same basic job—to remove unwanted or out-of-band signals—the specific job requirements of each filter vary depending on the given RF architecture and needs of the target device. In addition, the need for filtering is frequency-agnostic. While there's an overall trend for RF devices to operate at higher frequencies across applications, especially in the mobile telecom industry, it's not the requisite filtering jobs that are changing as much as the technologies needed for filtering at these higher frequencies.

AN OVERVIEW OF FILTERING JOBS ACROSS RF ARCHITECTURES

When designing a filter for an application that depends on receiving and sending RF signals, the first step is to identify the jobs that must be performed by the filter. These jobs can be very different depending on the RF architecture used in the application. Let's examine filtering tasks in three common RF architectures—superheterodyne (superhet), direct conversion, and direct sampling.

The superhet architecture is well-established and offers high performance over a wide range of frequencies, which makes it one of the most widely used radio receivers today. In this architecture, frequency mixing converts a received signal to a fixed intermediate-frequency (IF) signal to simplify processing *(Fig. 1)*.

Multiple RF filters take on several challenges in the superhet architecture, including:

- *Preselection:* A bandpass filter selects the spectrum range that contains the band of interest, allowing only the desired RF frequency to pass while suppressing the undesired spectrum.
- *Removing image spurs:* These are RF signals outside the band of interest that could mix with the LO and generate tones in the IF signal.
- *Removing IF spurs:* This is RF energy at the IF frequency that can show up as a tone in the IF.
- *Removing LO leakage:* This is radiation from the LO that can pass up and down the receiver chain. LO leakage could cause problems for the receive function as well as potential emission problems from the receiver itself.

While the superhet architecture is a proven and trusted approach, the large component count can impact size, weight, and power (SWaP), making it an impractical option for some RF applications. Therefore, in contrast to a

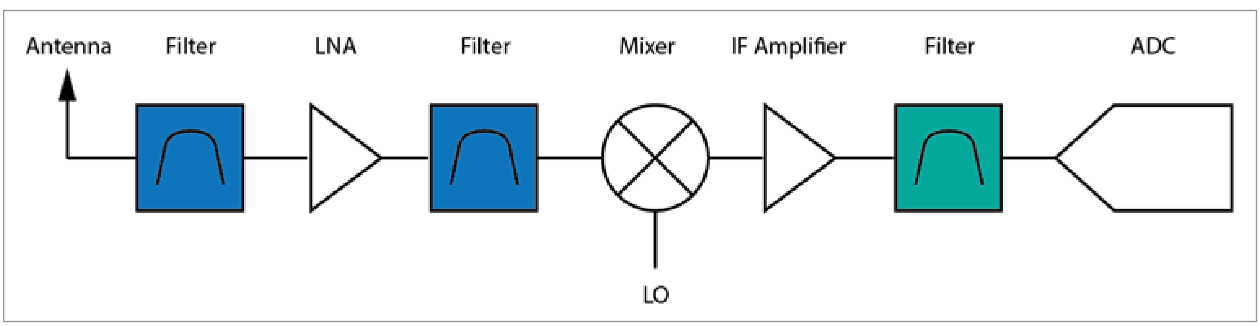

1. The functional block diagram for a superhet receiver shows the necessary components, which include multiple filters, a low-noise amplifier (LNA), a mixer, a local oscillator (LO), an IF amplifier, and an analog-to-digital converter (ADC).

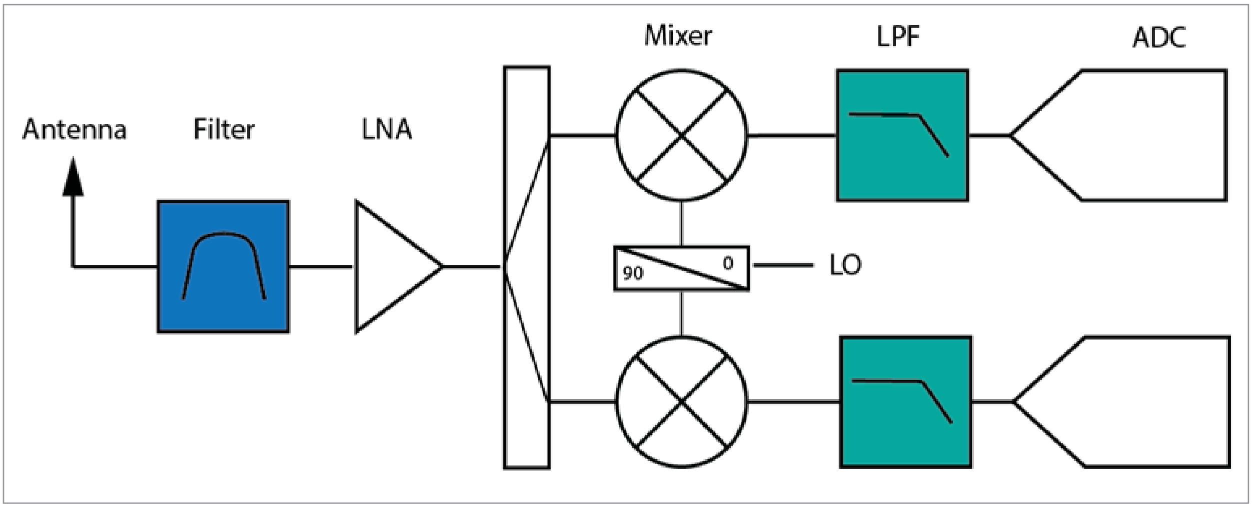

2. This DCR functional block diagram shows how the downconversion stage in a superhet receiver is replaced with an IQ demodulation step that takes the RF and feeds baseband to the ADC.

superhet, a direct-conversion receiver (DCR)—also known as a homodyne, synchrodyne, or zero-IF receiver—doesn't need to convert incoming signals to an IF signal. Instead, a DCR uses an LO with a frequency that's close to identical to the carrier frequency to demodulate the incoming signal via synchronous detection and generate the final baseband input to the analog-to-digital converter (ADC) *(Fig. 2)*.

In a DCR, the RF filter's jobs include preselection; preventing out-of-band signals from saturating the analog front end; and aliasing, which can be handled by a low-pass filter at baseband. This architecture is a good fit for applications that must maximize ADC bandwidth and need simplified wideband options from a SWaP standpoint. However, the need for I/Q balance and image rejection, and the potential for in-band harmonics, can make a DCR challenging to use in some applications.

Finally, the newest of these receiver architectures, the direct-sampling variety, is perhaps the holy grail of receiver architectures from a component simplicity standpoint. In direct sampling, the incoming signal is filtered to provide some selectivity and then amplified in an LNA with no mixing involved. Lastly, the RF signal is directly sampled by a fast ADC into digital form *(Fig. 3)*.

The jobs required of filters in a direct-sampling approach are like the jobs done in a DCR. They include preselecting, preventing out-of-band signals from saturating the analog front end, and aliasing with a bandpass filter to prevent interference in the alias bands of the ADC. While direct sampling is a

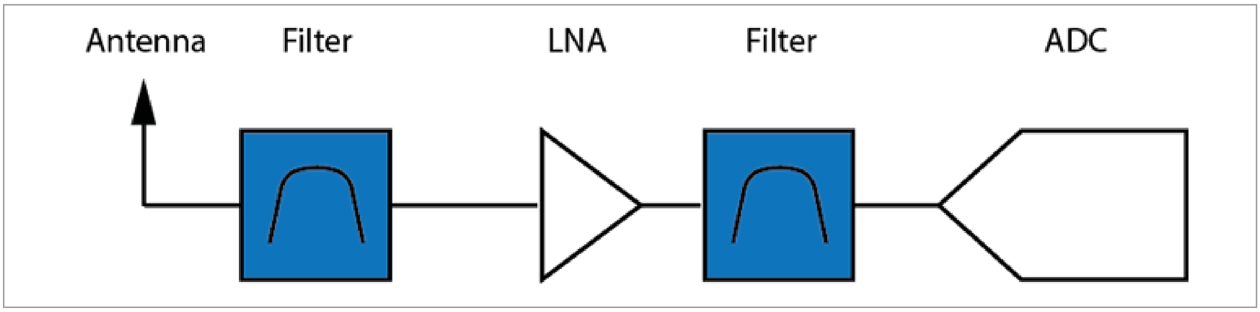

3. A greatly simplified architecture from a component perspective, the direct sampling architecture contains just the LNA, filters, and the ADC.

great option from a SWaP perspective, the approach presents some challenges, including bandwidth limitations by the ADC bandwidth at RF and the potential for gain imbalance.

TRENDS IN FILTER PERFORMANCE CONSIDERATIONS

Once the general job of a filter is determined based on the architecture at hand, it's time to think more specifically about the performance requirements for the filter based on the application it's being placed in. Let's look at a few industry-wide trends impacting filter performance decisions today.

Trend 1: It's not just about your application's current operating frequency.

As mentioned, the need for filters is frequency-agnostic—whether you're working on an electronic warfare system at 8 GHz or a 5G millimeter-wave (mmWave) system at 28 GHz, you'll need some level of filtering. Because no filter can operate across all frequencies, the appropriate filter for your application changes depending on if it's functioning at the low or high end of the spectrum *(Fig. 4)*.

But today, there are several reasons why it's not enough to simply consider the band your device is currently operating in. For example, let's look at mobile devices. One overarching trend is the shift to 5G. Currently, the 5G operating spectrum is divided into two frequency ranges—FR1, which covers 4.1 to 7.125 GHz and spans the L, S, and C bands; and FR2, which covers 24.25 to 52.6 GHz and includes the Ka band and beyond.

Because the availability of these bands is managed differently by region depending on where your end device will be used, the spectrum environment, or which frequencies are interacting with the band of interest, may change. How are operating frequencies managed in the United States? The Federal Communications Commission (FCC) holds auctions in which commercial concerns may purchase available frequencies. *Table 1* shows a list of recent and upcoming auctions.

Companies should be prepared to have different filtering requirements depending on which operating frequencies they purchased. In addition, their filter considerations will also change based on the type of applications operating at adjacent frequencies.

As more frequencies become available for devices to operate on, this trend of considering what's operating nearby gains more steam. For example, Earth Exploration-Satellite Services (EESS) operate globally between 23.6 and 24 GHz, which is directly adjacent to the 5G n258 band that operates between 24.25 and 27.5 GHz.

To prevent interference with the EESS, the International Telecommunication Union (ITU) placed limits on how much

TABLE 1: RECENT AND UPCOMING FCC FREQUENCY-SPECTRUM AUCTIONS

Auction	When	Frequency (GHz)
FCC Auction 101	Jan-19	28
FCC Auction 102	May-19	24
FCC Rules for 6 GHz Unlicensed	Apr-20	6.5
FCC Auction 103	May-20	39
FCC Auction 105	Aug-20	3.6
FCC Auction 107	~Dec-20	3.8
3GPP Release 17 (will include ~60 GHz unlicensed)	~Dec-21	60
FCC Auction TBD—DoD frequencies at 3.5 GHz switched to 5G	~Dec-21	3.5


5G

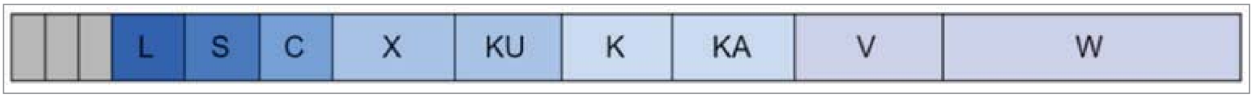

4. The diagram represents the bands from low to high frequency.

radiation may "leak" from 5G operations into the EESS band. Therefore, filters used in 5G devices operating at 24.25 GHz need high selectivity. This can be simplified if the filter technology is inherently high Q, which can also have the added benefit of reducing the complexity of the filter design required to reach a selectivity target.

Furthermore, in 2021, the 3.5-GHz band will be reallocated from military to telecom applications. As a filter designer, keeping an eye on trends, such as what is coming next in terms of available bandwidth, is important for being prepared to meet future filter needs.

As a filter designer, keeping an eye on trends, such as what is coming next in terms of available bandwidth, is important for being prepared to meet future filter needs.

Trend 2: Miniaturizing devices while also improving tolerance.

In general, depending on where RF filtering is deployed in the architecture, space will come at a premium. Like most industries, the trend in military and aerospace is to extend capabilities, such as rapidly sending and receiving more data, with a smaller footprint. Thus, more communication technology is being crammed into each satellite, which means the demand for smaller and lighter components is trickling down the supply chain.

Concurrently, in response to the ever-increasing demand for communications via satellite, satcom designers are pushing past the X and Ku bands to the higher-frequency Ka and V bands *(Table 2)*. As a result, there's a trend to shift from traditional heterodyne architectures to a direct RF sampling approach, which inherently changes the filtering tasks.

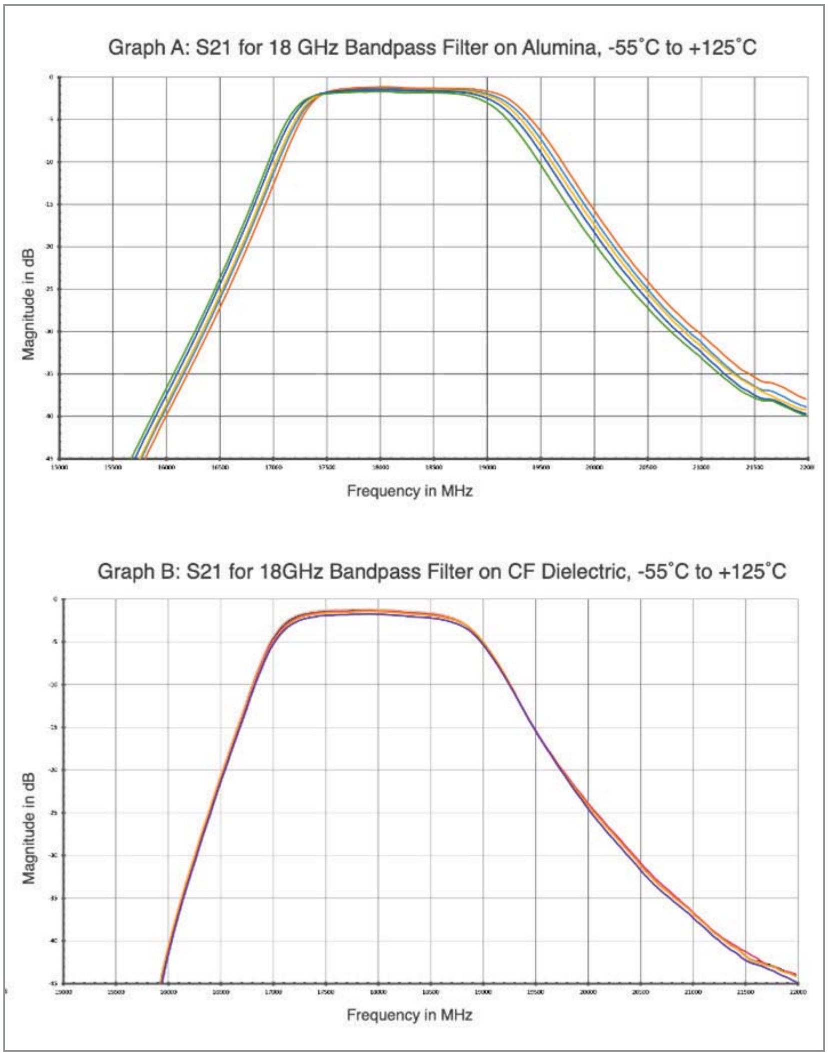

5. Graph A shows the response of microstrip bandpass filters built on alumina, while Graph B shows the response of microstrip bandpass filters built on Knowles Precision Devices' CF dielectric material.

Considering the importance of reducing mmWave filter size to keep up with the general trend of device miniaturization, manufacturing tolerance also plays a crucial role. Poor tolerance encroaches on potential board space or layers that could be used to add other devices or functionality. On top of that, tolerance not only affects filter specifications such as planned versus realized performance and potential loss of bandwidth, it also increases the cost of implementation.

In short, at mmWave especially, tolerance impacts can become significant and potentially alter the total cost of an implementation. If tolerance isn't considered during manufacturing, it can affect the yields of the overall system and further increase the need for guard banding, taking up useful spectrum space.

Trend 3: Managing temperature-stability issues.

As devices become smaller and denser, it becomes much more difficult to control temperature, which means systems will run hot and frequency variations may occur. Therefore, the emerging trend is for filters to perform within specification over a wide range of temperatures, with temperature stability of approximately 3 ppm/°C. By designing filters with the right dielectric material and filter topology, one may produce temperature-stable surface-mount filters with high rejection and low loss (*Fig. 5*).

PART 2 of our RF-filtering trends series will address current and emerging technologies that help meet the upcoming challenges in RF design work.

TABLE 2: COMMON MILITARY AND AEROSPACE APPLICATIONS OPERATING ACROSS VARIOUS BANDS

Band	Frequency Range	Typical Uses*
L	1 to 2 GHz	Military telemetry, GPS
S	2 to 4 GHz	Weather radar, surface ship radar, some satcom, GPS
C	4 to 8 GHz	Long-distance radio telecommunications
X	8 to 12 GHz	Satcom, radar
Ku	12 to 18 GHz	Satcom
K	18 to 26.5 GHz	Satcom, radar
Ka	26.5 to 40 GHz	Satcom
Q	33 to 50 GHz	Satcom
W	75 to 110 GHz	Satcom, military radar targeting and tracking applications

*Note that electronic-warfare applications also show up across all bands as adversaries look to detect and disrupt each other's systems.

DAVID VYE | Technical Marketing Director, Cadence

5G EVOLUTION Supports a New Wave of Wireless Services

Expanding 5G/6G connectivity to include network-to-smart device communications, combined with AI and IoT, will usher in a new industrial wave and offer greater business value for both industry and society.

The release of each new generation of wireless technology every decade or so has enabled mobile communication to progress considerably since the first portable phones appeared in the 1980s. Technical advances have created new services and business opportunities, driving what's being referred to as the third wave of communications. The evolution made possible through 5G and future 6G technology will support even more new services for industry and society, well into the 2030s and beyond *(Fig. 1)*.

5G represents the first step toward this next wave of services with expanded connectivity and a significant upgrade in multimedia capabilities combined with artificial intelligence (AI), machine learning (ML), and the Internet of Things (IoT). 5G will be the first generation of mobile communications to utilize millimeter-wave (mmWave) band frequencies, supporting bandwidths of several hundred megahertz and actualizing ultra-high-speed wireless data communications of many gigabits per second.

This article examines the expansion of 5G/6G wireless communications to new areas of service that will drive another industrial wave and offer greater business value for industry and society.

THE THIRD WAVE OF WIRELESS COMMUNICATIONS

5G and future systems will close the gap between the physical and cyber worlds. Today, mobile consumers use wireless connectivity to access the web from almost any location. In the future, high-speed coverage will be more widespread and faster, with greater emphasis on uplinking information from real-world events, either human and/or IoT, to the internet.

Once this information is in the cloud, AI could reproduce the real world in cyberspace and emulate it beyond physical, economical, and time constraints, so that "future prediction" and "new knowledge" can be discovered and shared. The role of wireless communications in this cyber-physical fusion is assumed to include high-capacity and low-latency trans-

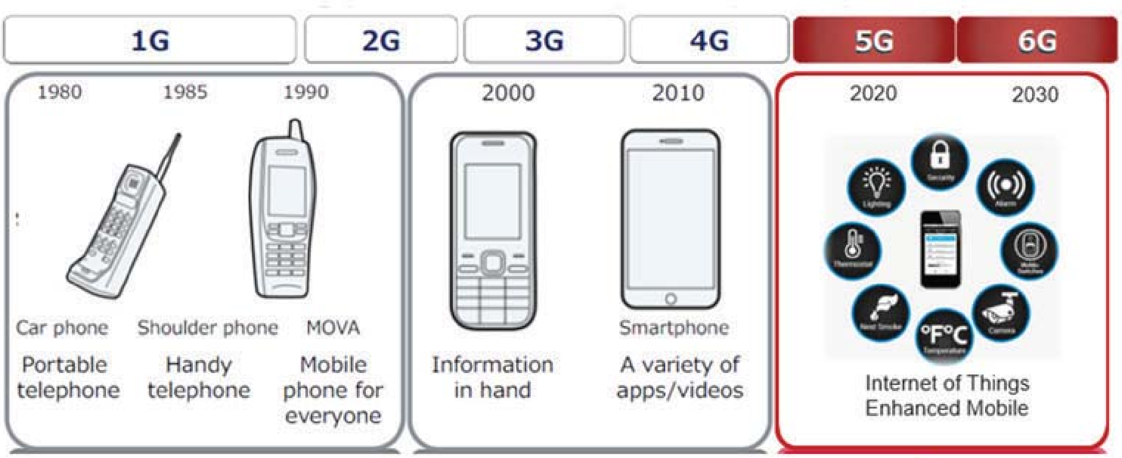

1. There have now been five generations of mobile communications technology and services, with a sixth on the way.

mission of real-world images and sensing information, and feedback to the real world through high-reliability and low-latency control signaling.

Radio communications in this cyber-physical fusion scenario correspond to the role of the nervous system transmitting information between the brain and the body. Communications convert real-world events to the cyber world through enhanced uplink capabilities and provide feedback information to humans and devices through low-latency downlink functionality.

NEXT-GENERATION AREAS OF SERVICE

The next wave of communications focuses on three areas of service *(Fig. 2)* including:

- Enhanced mobile broadband (eMBB), which extends the current mobile experience with high data throughput on the order of more than 10 Gb/s, high system capacity on the order of more than 1000X that of LTE, and a much better spectral efficiency (3-4X) than LTE. Its use cases are high-speed mobile broadband, virtual reality, augmented reality, gaming, and more.
- Ultra-reliable, low-latency communications (URLLC), which focuses on achieving low latency, high reliability, and high availability. The expectation is for latencies of less than 1 ms. This is basically for mission-critical use cases and applications.
- Massive machine-type communications (mMTC), which provides connectivity to a huge number of devices whose traffic profile is typically a small amount of data (spread) sporadically. Consequently, latency and throughput aren't a big concern. The main concern is the optimal power utilization of those devices because they're battery-powered and the expectation of battery life is around 10 years or so.

Current activity in mmWave front-end design, including antenna-in-package (AiP) phased arrays *(Fig. 3 on page 24)*, large-scale beamforming RF integrated circuits (RFICs), multi-technology integration, and system-level electromagnetic (EM) analysis will all contribute to realizing New Radio (NR) access technology that can be cost effective and easy to install. This will support the small-cell networks that achieve 5G/6G performance.

Early 5G deployment and related trials have shown room for improvement in coverage and uplink performance in non-line-of-sight (NLOS) environments and heavy traffic use cases. While future system performance goals are still in the early phases of consideration, full realization of the promise of this next wave of communications creates a need for continued enhancements. Extreme performance is necessary to provide the high reliability and low latency called for by mission-critical (time-sensitive) applications such as self-driving vehicles.

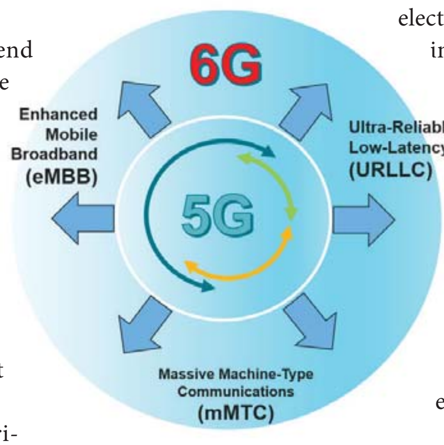

2. These are some of the new business services that will be enabled with the third wave of communications, which has been initiated with the advent of 5G.

6G PERFORMANCE GOALS

6G will implement many different technologies to achieve its performance goals. Among them will be new topologies of overlapping cells with distributed networks of beamforming antennas controlled by AI and ML to dynamically select optimum transmission paths. Previous cellular communications were based on networks of hexagonal cells spaced far enough apart to avoid signal interference with neighboring cells. In the future, there will be overlapping cells that can be dynamically reconfigured. In addition, coverage will expand through space, sea, and high-altitude drones.

New functionality in spatial multiplexing and massive multiple-input multiple-output (mMIMO) are under investigation, including the use of reflective surfaces and metamaterials to manage signal propagation in crowded urban environments with limited LOS. 6G may employ a spatially non-orthogonal, overlapped, and dynamic topology to increase path selection. Beam control through AI and ML will help reduce intercell interference at a cost of complexity.

Besides reconfiguring networks, much of the 5G/6G focus will be on physical design of radio access front ends. Strategic design partitioning, leveraging of optimal semiconductor processes, and multi-fabric assemblies will undoubtedly be utilized, calling for a range of simulation technologies, design and manufacturing flows, and tool interoperability. These trends will require software design support for co-design and co-optimization of next-generation wireless electronic systems across multiple domains—including RF, analog, and digital simulation—aided by large-scale EM and thermal analysis, and robust design verification and signoff.

A common RFIC and system-in-package (SiP) design challenge is concerned with how RF intellectual-property (IP) blocks are subject to EM, capacitive, supply, and substrate coupling. These potentially harmful interactions result from effects that occur with high-frequency signaling. Noise, either into or out of a block, can travel through the substrate or through power bussing. Placement (floorplanning) of noise-generating and noise-sensitive blocks is design critical.

Parasitic coupling capacitance within/between RF blocks, and signals routed nearby (100s to 1000s of microns away) can cause disrupted performance. Self-inductance of any nets connected to the RF block, and mutual inductance between any net within an RF block to nets in neighboring blocks, is another concern.

RF IP blocks interact much differently than digital IP blocks. Most place-and-route tools aren't able to address the unique issues confronted in integrating RF IP. An RF engineer working with RF-aware design tools is required to successfully integrate blocks at the chip, package, or board levels. To understand the effects of parasitic coupling, either capacitive, inductive, and through the substrate, closed-form distributed transmission-line models and EM analysis are essential for RF IP development.

Using higher-frequency bands in 6G (94 GHz to 3 THz) will help reduce the size of these antennas, making efforts to shrink component footprints easier. However, the antennas, feed networks, and package interconnects will all be more susceptible to parasitics and unintended coupling (crosstalk), requiring rigorous EM analysis and design verification. This move to higher spectrum will lead to a wide range of design and integration challenges.

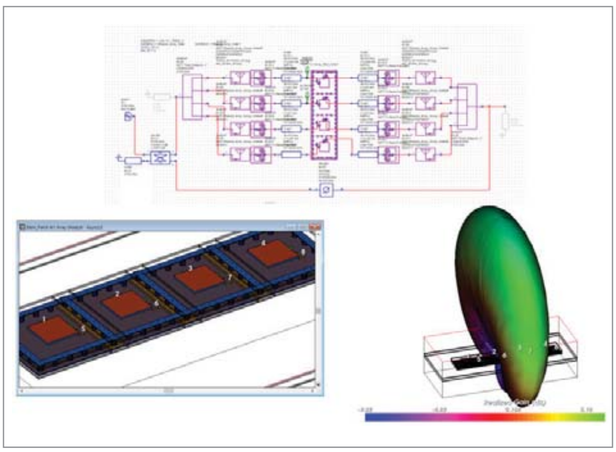

3. The images depict dual-polarized AiP phased-array technology designed in Cadence AWR Design Environment software.

NEED FOR WIRELESS TECHNOLOGY IMPROVEMENTS

5G deployment and related trials have shown there's room and need for improvements to the coverage and uplink performance of NLOS environments and heavy-traffic use cases. To fully achieve the promise of this next wave of communications, we'll need continued enhancements to guarantee the high reliability and low latency necessary to close the gap between the cyber and physical worlds. 5G evolution will concentrate on better uplinking and toward more delivery guarantees, as opposed to "best effort," with a focus on URLLC *(Fig. 4)*.

Achieving URLLC performance with < 1-ms latency and up to "nine nines" (99.9999999%) mission-critical reliability (for factory operational technology) for networks based on edge cloud computing will require a massive number of small-cell radio access points and distributed antennas with AI/ML controlled beamsteering. Implicit in the requirements for this vast deployment of non-orthogonal networks will be the need to drive down the cost of the beamforming antenna arrays and complex receivers, especially if faster-than-Nyquist signaling techniques are applied, while greatly improving (beyond the current best effort) uplink technology.

CONCLUSION

A key goal of 5G has been to expand the reach and value of wireless technology beyond the individual mobile subscriber in support of mMTC and URLLC. Expanding connectivity to include network-to-smart device communications, combined with AI and IoT, will usher in a new industrial wave and offer greater business value for both industry and society. mw

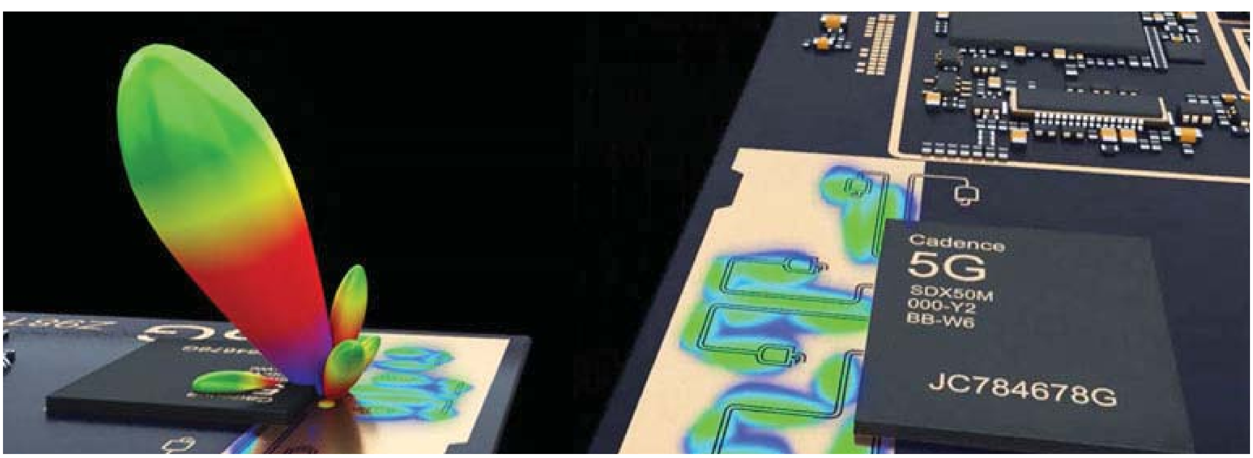

4. Integration of beamsteering RF front-end module technologies will improve uplink data rates for 5G/6G devices.

26 TO 86 GHZ

mmWave Components

400+ Models and Counting

- In-house design and manufacturing capability
- Industry-leading quality
- Supply chain security—no EOL target through the life of your system

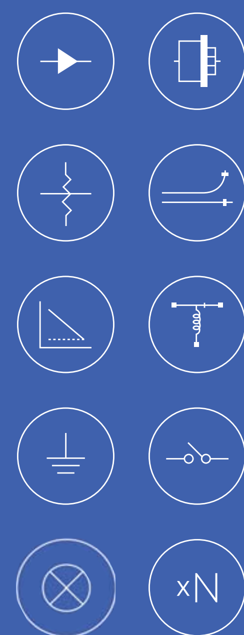

Mini-Circuits®

CHRIS DeMARTINO | Sales and Applications Engineer, Modelithics Inc.

Accurate Models and Discrete Part-Value Optimization Combine to Improve Workflows

A workflow that combines measurement-based models with discrete part-value optimization can aid designers by automatically adjusting a design's component values to optimal manufacturer part values.

Designing RF filters and other high-frequency circuits with today's simulation software tools often involves performing some form of optimization to achieve the desired performance. For example, take the case of a lumped-element filter. Optimizing such a filter involves adjusting the values of its lumped components until the filter achieves an optimal frequency response.

However, once the component values have been determined via optimization, they may still need to be adjusted to the closest discrete, or "real-life," manufacturer part values. Depending on the design's complexity, this extra step can create a bit of extra legwork for the designer.

Fortunately, with the proper tools, it's possible to perform discrete part-value optimizations in which component values are directly adjusted to optimal manufacturer part values. This optimization method eliminates the need for designers to manually adjust optimized component values to the closest available real-life part values, thereby cutting one step from the overall design process.

This article explains how a discrete part-value optimization method can be leveraged to develop a lumped-element bandpass filter designed using the Cadence AWR Design Environment (AWRDE). The design includes Modelithics measurement-based passive-component models, which enable simulations to accurately predict the filter's real performance. After completing an initial filter design, a discrete part-value optimization achieves the desired frequency response. The article wraps up by comparing measured data to the simulated results.

BEGINNING WITH THE iFILTER SYNTHESIS MODULE

The AWRDE consists of several software tools used for developing RF/microwave products. Among them are Microwave Office for RF/microwave circuit design and the AXIEM 3D planar electromagnetic (EM) simulator. For this design example, we used both tools.

Various add-on modules can also be utilized within the AWRDE platform. One of them is iFilter, an integrated synthesis wizard used to develop RF/microwave filters.

For this example, we used iFilter to start the design process. We specified the Passband as Bandpass and the Realization as Lumped. Following these selections, we chose Narrowband Lumped Filter as the Main Filter Type. Subsequently, we selected Inductive (identical shunt C) from the list of options.

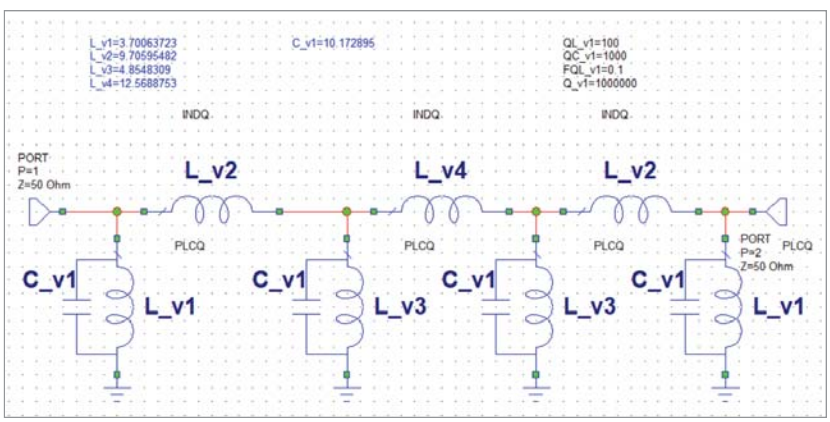

1. Using iFilter to generate the filter design results in this Microwave Office schematic. The bold reference designations that correspond to the variables were added for illustration purposes.

The next user interface contains the filter schematic, frequency response, and several user-defined parameters. For this design example, we specified a Chebyshev filter with a center frequency of 950 MHz and bandwidth of 300 MHz.

We can then automatically create a new schematic of the filter in Microwave Office *(Figure 1)*. Note that the tool automatically set several variables. *Table 1* lists these variables and their corresponding values; *Figure 2* shows the filter's simulated frequency response.

INCORPORATING MICROSTRIP TRANSMISSION LINES AND MODELITHICS MODELS

While the schematic shown in *Figure 1* represents a good starting point for the design, the overall design process is far from complete. For one, to properly model a real filter, one must add microstrip interconnects to the schematic.

We must also consider component modeling. In the schematic shown in *Figure 1*, the inductor and capacitor models are ideal closed-form elements with user-defined quality-factor (Q) parameters.

Alternatively, utilizing Modelithics measurement-based inductor and capacitor models makes it possible to predict the filter's performance more accurately. The company's models offer the benefit of both part-value and substrate scalability. These models accurately capture substrate-dependent parasitic behavior and offer advanced pad features for accurate EM/circuit co-simulations. Hence, we used Modelithics inductor and capacitor models in place of the ideal elements seen in *Figure 1*.

Figure 3 shows a new filter schematic created by duplicating the original one. This new schematic contains all the necessary microstrip interconnects and vias. In addition, the ideal inductor and capacitor models are replaced with Modelithics models.

Table 1

L_v1	3.70063723 nH
L_v2	9.70595482 nH
L_v3	4.8548309 nH
L_v4	12.5688753 nH
C_v1	10.172895 pF

These variables generated by iFilter represent the part values of the inductors and capacitors.

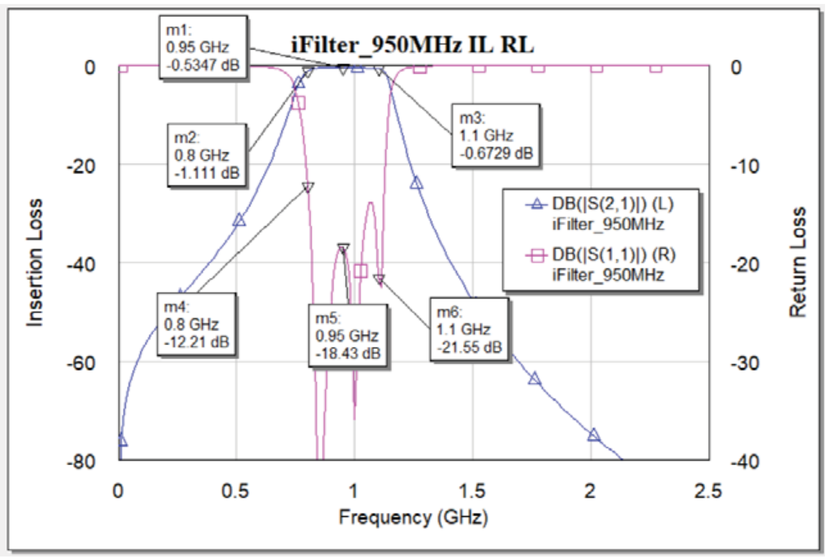

2. The simulated frequency response reveals a center frequency of 950 MHz.

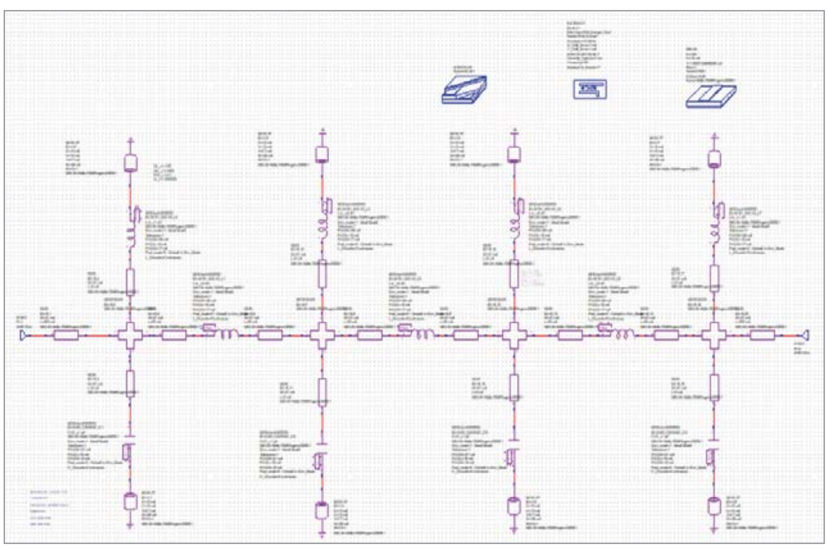

3. The new filter schematic incorporates microstrip interconnects and vias along with Modelithics passive-component models.

For this example, we chose the Würth Elektronik WE-KI 0402-size inductors for all the inductors. For the capacitors, we used Kemet's CBR04C 0402-size capacitors. Furthermore, the substrate used for this filter is 10-mil-thick Rogers RO4350B.

The schematic shown in *Figure 3* also includes an EXTRACT block and a STACKUP multi-layer substrate definition. We added these elements to the schematic via the Create_Stackup script.

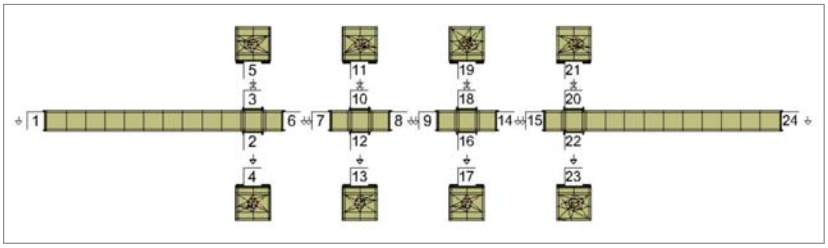

4. We extracted this EM structure with the help of the Create_Stackup script.

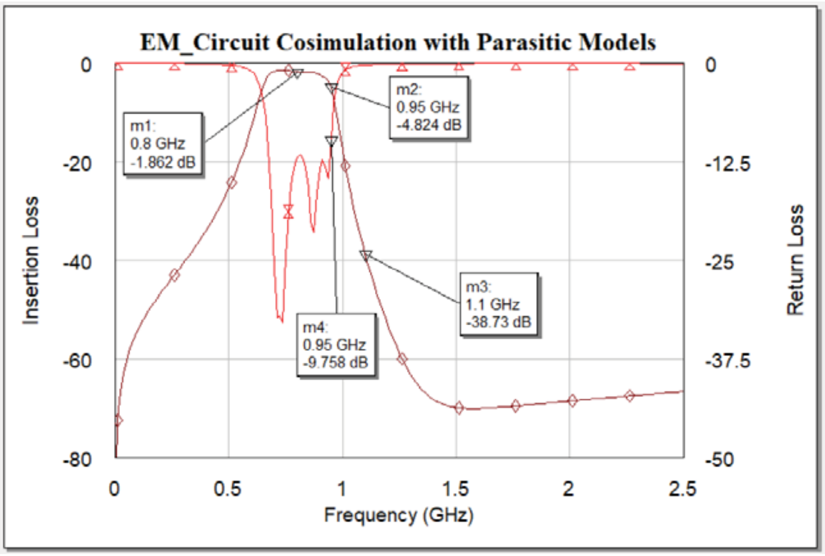

5. Adding microstrip elements and Modelithics models results in a downward shift in frequency and greater passband insertion loss.

```
installDir="C:\Program Files (x86)\AWR\Foundry\Modelithics"
dataDir=installDir + "\Data\"

L_vector=vfile(dataDir + "IND_WTH_0402_002.txt")
C_vector=vfile(dataDir + "CAP_KMT_0402_004.txt")

L_v1=L_vector[8]=3.6
L_v2=L_vector[20]=9.5
L_v3=L_vector[11]=4.7
L_v4=L_vector[24]=13

C_v1=C_vector[100]=10
```

6. Adding these equations to the Microwave Office schematic enables the appropriate .txt files to be the basis for a discrete part-value optimization.

These two elements together facilitate EM/circuit co-simulation by creating and configuring a metal geometry from the PCB layout of selected schematic elements.

In this case, we selected all the microstrip interconnects and vias for extraction. Therefore, these elements will be analyzed with the AXIEM EM simulator. The inductors and capacitors will be analyzed within the Microwave Office circuit simulator. *Figure 4* shows the extracted EM structure comprising all the interconnects and vias.

Now that the EM extraction is properly configured, we can perform an EM/circuit co-simulation by simulating the schematic shown in *Figure 3*. This schematic includes the same variables found in the original schematic *(Table 1, again)*. The inductor and capacitor values of the Modelithics component models are set to the same variables as the corresponding components in the original schematic, meaning the component values are unchanged.

Setting the Sim_mode parameter of all Modelithics models to 0 enables them to behave as full parasitic models, thus accounting for all real-world parasitic, pad, and substrate effects. *Figure 5* shows the frequency response after simulating the filter with Sim_mode set to 0 for all models. It's evident that the response shifted downward in frequency and is more lossy compared to the results shown in *Figure 2*. The filter also falls short of achieving the desired 300-MHz bandwidth.

DISCRETE PART-VALUE OPTIMIZATION TO THE RESCUE

Because the filter doesn't currently meet the design goals, the next step is to perform a discrete part-value optimization. This optimization technique will directly adjust the inductor and capacitor values to the optimal part values in the Würth Elektronik WE-KI and Kemet CBR04C part families, respectively.

To facilitate performance of discrete part-value optimizations in the AWRDE, Modelithics offers .txt files for all passive-component models. Each file contains a list of all manufacturer part values in the part family represented by the model. These files are located in the <installDir>\Modelithics\Data folder, where <installDir> is the installation folder (C:\Program Files (x86)\AWR\Foundry by default). The IND_WTH_0402_002.txt file contains all part values in the Würth Elektronik WE-KI family of inductors, while the CAP_KMT_0402_004.txt file contains the same information for the Kemet CBR04C capacitor family.

Figure 6 displays the equations that must be added to the Microwave Office schematic *(Figure 3, again)* to utilize these files for a discrete part-value optimization. The equations shown are based on the default file locations. Note that the IND_WTH_0402_002.txt and CAP_KMT_0402_004 .txt files generate two vectors, L_vector and C_vector, respectively. As a result, the L_vector element contains each of the part values in the Würth Elektronik WE-KI part family, while the C_vector element contains each of the part values in the Kemet CBR04C part family.

From the values shown in the bottom portion of *Figure 6,* we can see that the variables are no longer equal to the initial values of *Table 1*. Rather, they're now set to the vector indices that correspond to the manufacturer part values closest to the initial values. *Table 2* lists these manufacturer part values.

It's now time to perform a discrete part-value optimization. To do so, we specify the variables L_v1, L_v2, L_v3, L_v4, and C_v1 for optimization in the Variable Browser. Next, we set the optimization goals. Over the passband of 800 to 1100 MHz, we're shooting for an S_{21} value greater than –2 dB and an S_{11} value less than –12 dB. For the lower and upper rejection bands, the goal is an S_{21} value of less than –20 dB. Finally, upon opening the optimization user interface, the user must select Discrete Local Search from the list of optimization methods.

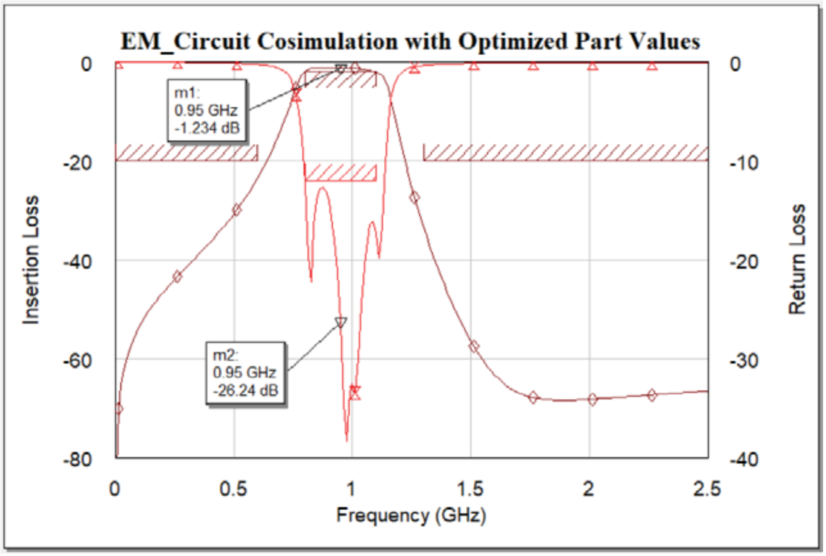

7. Shown is the filter's post-optimization frequency response. The response reveals a center frequency of 950 MHz along with the desired bandwidth.

Table 2

L_v1	3.6 nH
L_v2	9.5 nH
L_v3	4.7 nH
L_v4	13 nH
C_v1	10 pF

Shown are the manufacturer part values that are closest to the initial values.

Table 3

L_v1	3.6 nH
L_v2	9 nH
L_v3	5.6 nH
L_v4	11 nH
C_v1	7.0 pF

These are the final optimized manufacturer part values.

Figure 7 shows the filter's simulated frequency response after performing the discrete part-value optimization, while *Table 3* lists the optimized manufacturer part values. Now that the filter performs well, the design process is complete.

MEASURED DATA VERSUS SIMULATED RESULTS AND CLOSING

The final step is to validate the design by building and measuring the filter. We assembled two filters using the same Würth Elektronik WE-KI inductors and Kemet CBR04C capacitors from the final simulation. *Figure 8* shows the measured data of both filters along with the final simulated results. The measured data agrees with the simulated results, thereby validating the design process.

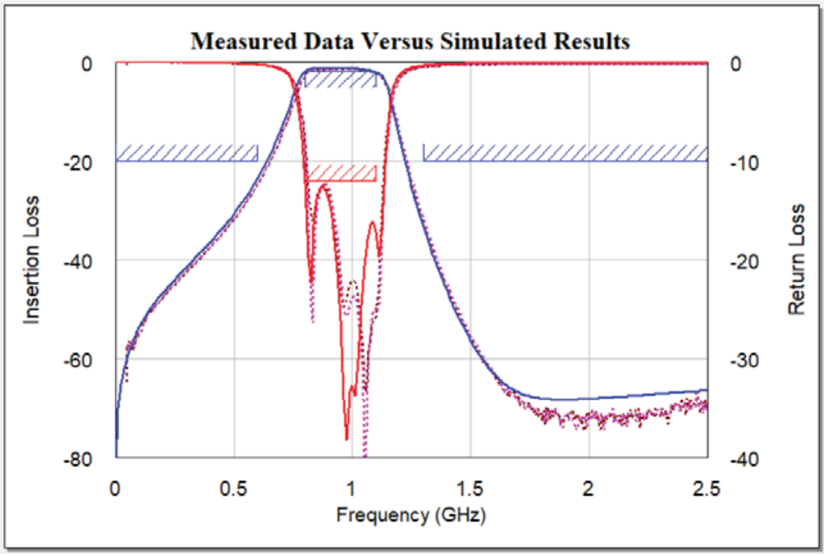

8. The measured data for S_{21} and S_{11} (dashed traces) largely agreed with the corresponding final simulated results (solid traces).

In closing, utilizing Modelithics measurement-based models combined with a discrete part-value optimization method within the Cadence AWR Design Environment can be an effective way to design RF/microwave circuits. The approach pinpoints exactly which manufacturer part values are best suited for a design. mw

PETER DELOS, BOB BROUGHTON, JON KRAFT | Analog Devices

Phased-Array Antenna Patterns (Part 4)—GRATING LOBES

This latest installment in the series examines the topic of grating lobes with a focus on element spacing.

In the first three parts of this series, we introduced the phased-array steering concept and looked at the influencers on array gain. In the next two parts, we'll discuss grating lobes and beam squint. Grating lobes can be hard to visualize, so we'll draw on their similarity with signal aliasing in digital converters, then use that to think of a grating lobe as a spatial alias.

In the upcoming Part 5, we'll explore the issue of beam squint. Beam squint is an unfocusing of the antenna across frequency when we use phase shift, instead of a true time delay, to steer the beam. We'll also discuss the tradeoff between these two steering methods and understand the impact of beam squint on typical systems.

AN INTRODUCTION TO GRATING LOBES

So far, we have only examined the case in which the element spacing is $d = \lambda/2$. *Figure 1* begins to illustrate why an element spacing of $\lambda/2$ is such a common metric in phased arrays. Two cases are shown. First, in blue, we show the same 30° plot from Part 3 of this article series *(October 2020 Microwaves & RF)*. Next, the d/λ spacing is increased to 0.7 to show how the antenna pattern changes.

With this increase in spacing, note the reduction in the beamwidth, which is a positive result. The decreased spacing of nulls brings them closer together, which is also an acceptable result. But now there's a second angle, in this case at –70°, where there's full array gain. This is a most unfortunate result. This replica of antenna gain is defined as a grating lobe and can be considered spatial aliasing.

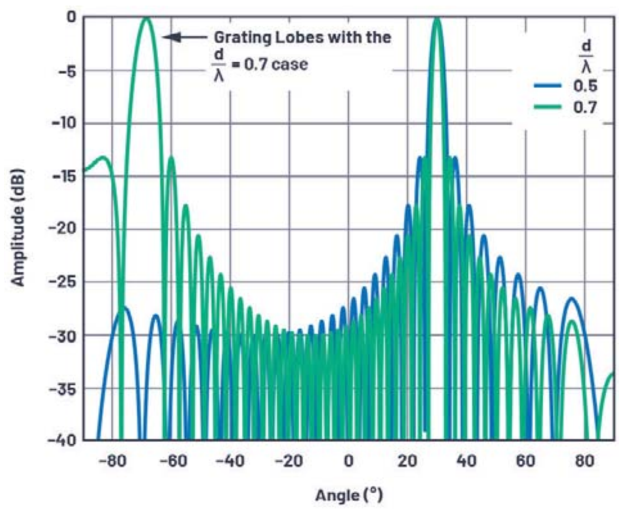

1. This plot illustrates the normalized array factor of a 32-element linear array at two different d/λ spacings.

ANALOGY TO SAMPLED SYSTEMS

An analogy useful in visualizing grating lobes is to think of aliasing in a sampled system. In an analog-to-digital converter (ADC), undersampling is often used when frequency-planning a receiver architecture. Undersampling involves purposefully reducing the sample rate (fS) such that the sampling process translates frequencies above fS/2 (the higher Nyquist zones) to appear as aliases in the first Nyquist zone. This causes those higher frequencies to appear as if they were at a lower frequency at the output of the ADC.

A similar analogy can be considered in phased arrays, where the elements spatially sample the wavefront. The Nyquist theorem can be extended to the spatial domain if we suggest that two samples—that is, elements—per wavelength are required to avoid aliasing. Therefore, if the element spacing is greater than $\lambda/2$, we can consider this spatial aliasing.

CALCULATING WHERE GRATING LOBES APPEAR

But where will these spatial aliases (grating lobes) appear? Previously, we showed the phase shift applied to the elements across the array as a function of beam angle:

$$\Delta\Phi = \frac{2\pi d sin\theta}{\lambda} \qquad (1)$$

Inversely, we can compute the beam angle as a function of phase shift:

$$\theta = arcsin\left(\frac{\Delta\Phi}{2\pi} \times \frac{\lambda}{d}\right) \qquad (2)$$

The arcsin function only produces real solutions for arguments between −1 and +1. Outside of these bounds, the solution isn't real—the familiar "#NUM!" in spreadsheet software. Also note that the phase in Equation 2 is periodic and repeats every 2π. So, we could replace ΔΦ with (m × 2π + ΔΦ) in the beamsteering equation to yield Equation 3:

$$\theta = arcsin\left(\frac{m \times 2\pi + \Delta\Phi}{2\pi} \times \frac{\lambda}{d}\right) \qquad (3)$$

where m = 0, ±1, ±2, …

To avoid grating lobes, our goal is to obtain a single real solution. Mathematically, this is accomplished by keeping:

$$\left|\frac{m \times 2\pi + \Delta\Phi}{2\pi} \times \frac{\lambda}{d}\right| > 1 \text{ for all } m \geq 1 \qquad (4)$$

If we do so, then all of the spatial images (that is, m = ±1, ±2, etc.) will produce nonreal arcsin results, and we can ignore them. But if we can't do this, and therefore some values of m > 0 produce real arcsin results, then we end up with multiple solutions: grating lobes *(Fig. 2)*.

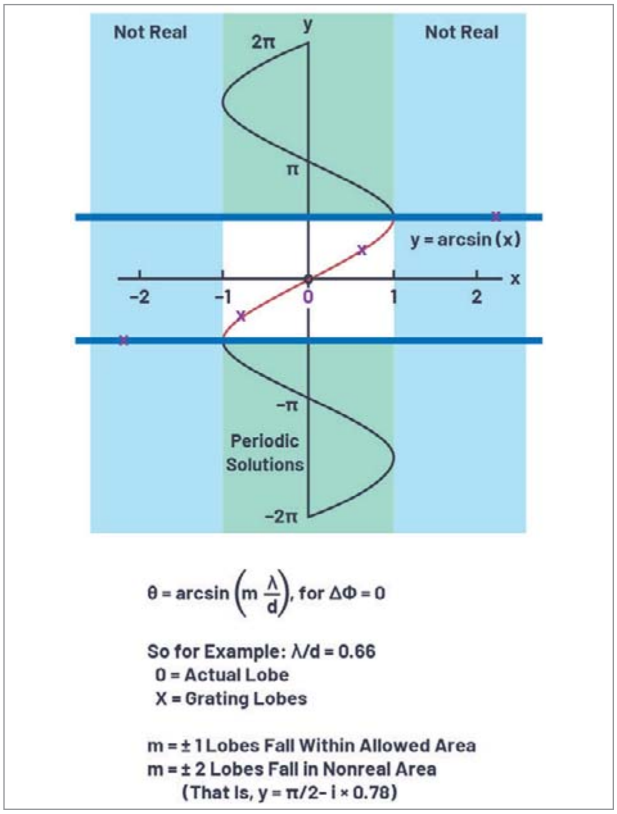

2. Shown is the arcsin function application to grating lobes.

GRATING LOBES FOR d > λ AND λ = 0°

Here are some examples to better illustrate this scenario. First, consider the case at mechanical boresight where θ = 0, and therefore ΔΦ = 0. Then Equation 3 simplifies to Equation 5:

$$\theta = arcsin\left(m \times \frac{\lambda}{d}\right), for\ \Delta\Phi = 0 \qquad (5)$$

From this simplification, it's evident that if λ/d is > 1, then only m = 0 could give an argument that's bounded between −1 and +1. And that argument will just be 0, and the arcsin(0) = 0°, the mechanical boresight angle. So, this is all as we would expect. Furthermore, for any m ≥ 1, the arcsin argument will be too large (>1) and the resulting answer will not be real. We will see no grating lobes for θ = 0 and d < λ!

However, if d > λ (therefore, λ/d is <1), then multiple solutions—grating lobes—could exist. For example, if λ/d = 0.66 (that is, d = 1.5λ), then real arcsin solutions would exist for m = 0 and for m = ±1. That m = ±1 is the second solution, which is the spatial aliasing of the desired signal. Therefore, we can expect to see three main lobes, each with approximately equal amplitude, located at arcsin(0 × 0.66), arcsin(1 × 0.66), and arcsin(−1 × 0.66). In degrees, these angles are 0° and ±41.3°. In fact, this is what our array factor plot shows in *Figure 3*.

GRATING LOBES FOR λ/2 < d < λ

In simplifying the grating-lobe equation (Equation 5), we chose to only look at mechanical boresight (ΔΦ = 0). And we saw that, at mechanical boresight, grating lobes would not appear for d < λ. But from our analogy of sampling theory, we know that we should also expect to see some kind of grating lobe for any spacing greater than λ/2. So where are the grating lobes for λ/2 < d < λ?

First, recall how the phase changed with steering angle in *Figure 4* from Part 1 of this article series *(July 2020 Microwaves & RF)*. We saw ΔΦ range from 0 to ±π as the main lobe deviated from mechanical boresight. Therefore:

$$\frac{m \times 2\pi + \Delta\Phi}{2\pi} \times \frac{\lambda}{d} \qquad (6)$$

will range:

$$\text{from 0 to}\left(\pm 0.5 \times \frac{\lambda}{d}\right) for\ m = 0 \qquad (7)$$

And for |m| ≥ 1, it will always be something beyond:

NEL FREQUENCY CONTROLS, INC.

Your Silent Partner®

Phase Locked Clean Up ULPN VCXO

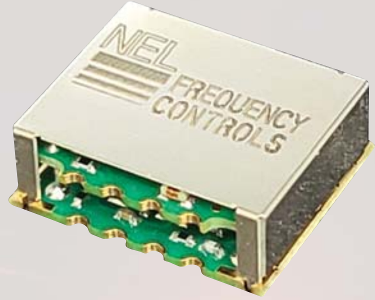

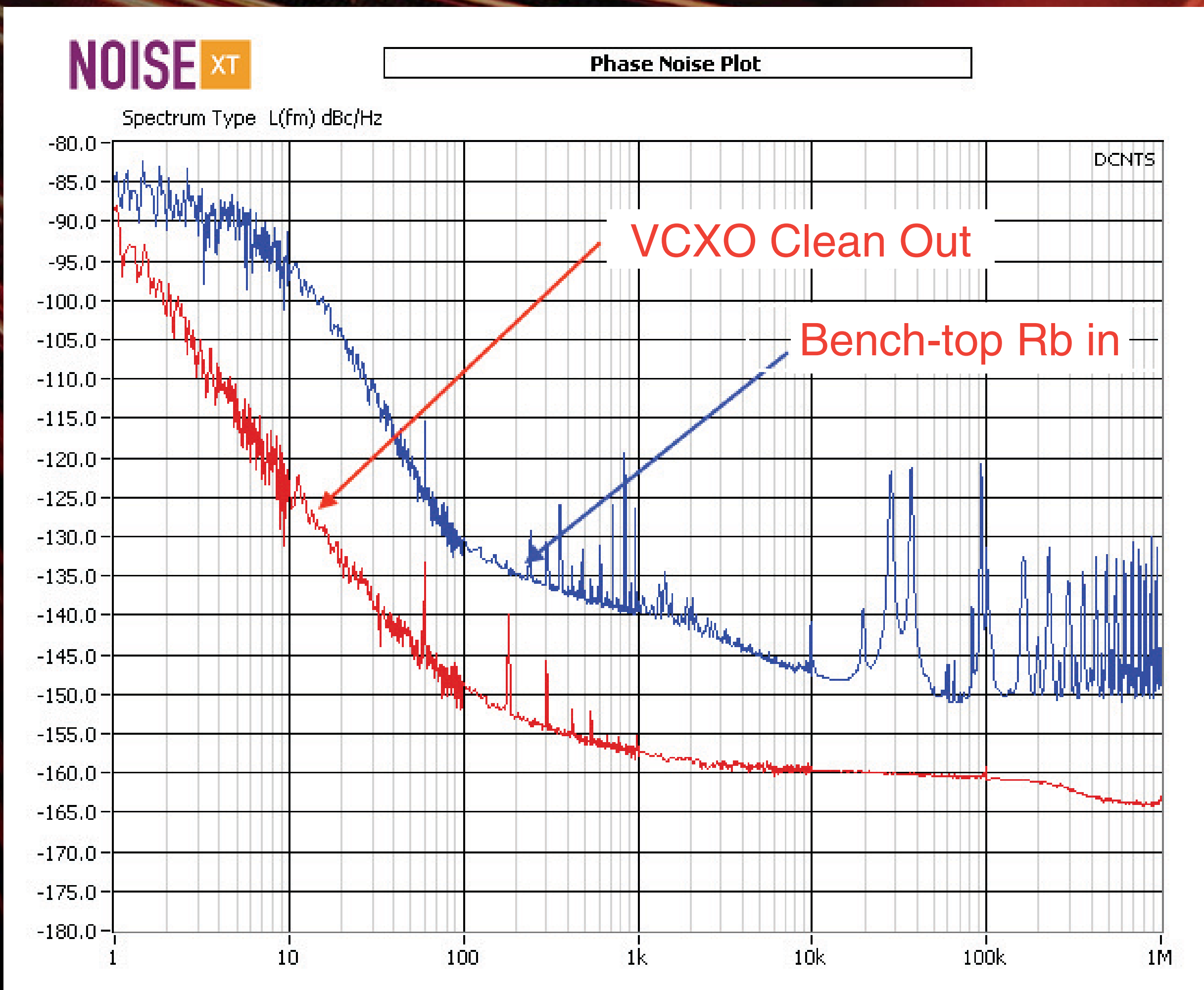

Features

- Low G sensitivity
- Low phase noise similar to OCXO
- 17x14mm Compact SMD Package
- Low power consumption independent on ambient temperature and no warm up
- Fast ready

Applications

- Significantly improves Phase Noise of incoming signal
- Atomic Clocks, GNSS Based Clocks
- Test and Measurement
- COTS/Dual use

Contact Us Today **www.nelfc.com** | **262.763.3591** | **sales@nelfc.com**

$$\pm 0.5 \times \frac{\lambda}{d} \qquad (8)$$

This restricts the minimum permissible λ/d if we want to keep the entire arcsin argument > 1 for all |m| ≥ 1. Consider two cases:

If λ/d ≥ 2 (that is, d ≤ λ/2), then you could never have multiple solutions, regardless of the value of m. All m > 0 solutions will result in an arcsin argument > 1. This is the only way to avoid grating lobes to the horizon.

But if we purposefully restricted ΔΦ to something less than ±π, then we could tolerate a smaller λ/d and still not see grating lobes. Reducing the range of ΔΦ means reducing the maximum steering angle of our array. It's an interesting tradeoff that will be explored in the next section..

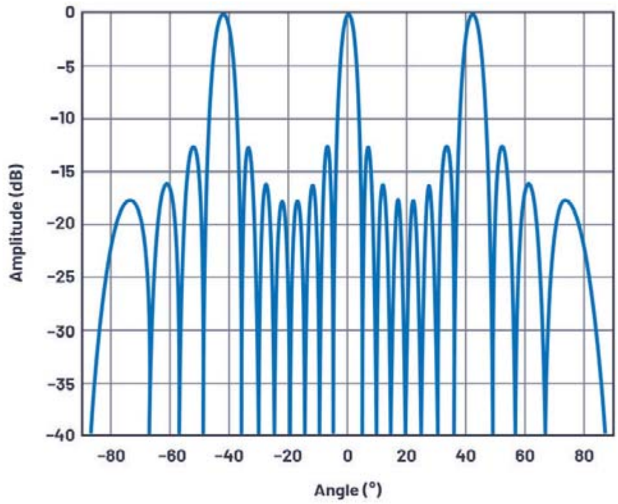

3. An array factor plot at boresight for d/λ = 1.5, N = 8 shows three main lobes at angles of 0° and ±41.3°.

ELEMENT SPACING CONSIDERATIONS

Should the element spacing always be less than λ/2? Not necessarily! This becomes a tradeoff for the antenna designer to consider. If the beam is steered completely to the horizon, then θ = ±90°, and an element spacing of λ/2 is required (if no grating lobes are allowed in the visible hemisphere). But in practice, the maximum achievable steering angle is always less than 90°. This is due to the element factor and other degradations at large steering angles.

From the arcsin figure *(Fig. 2, again)*, we can see that if the y axis, θ, is restricted to a reduced limit, then grating lobes only occur at scan angles that aren't used anyway. What would this reduced limit (θmax) be for a given element spacing (dmax)? We had said previously that our goal is to keep:

$$\left| \frac{m \times 2\pi + \Delta\Phi}{2\pi} \times \frac{\lambda}{d} \right| > 1 \text{ for all } |m| \geq 1 \qquad (9)$$

We can use this to calculate where our first grating lobe (m = ±1) would appear. Making this change, and using Equation 1 from Part 1 for ΔΦ, gives:

$$\frac{\pm 1 \times 2\pi + \frac{2\pi d_{max} sin\theta_{max}}{\lambda}}{2\pi} \times \frac{\lambda}{d_{max}} = 1 \qquad (10)$$

Which simplifies to:

$$\pm\lambda + d_{max} sin\theta_{max} = d_{max} \qquad (11)$$

Then solving for dmax:

$$d_{max} = \frac{\lambda}{1 + |sin\theta_{max}|} \quad for\ \theta_{max}\ from\ 0\ to\ \pm\pi/2 \qquad (12)$$

This dmax is the condition for no grating lobes in the

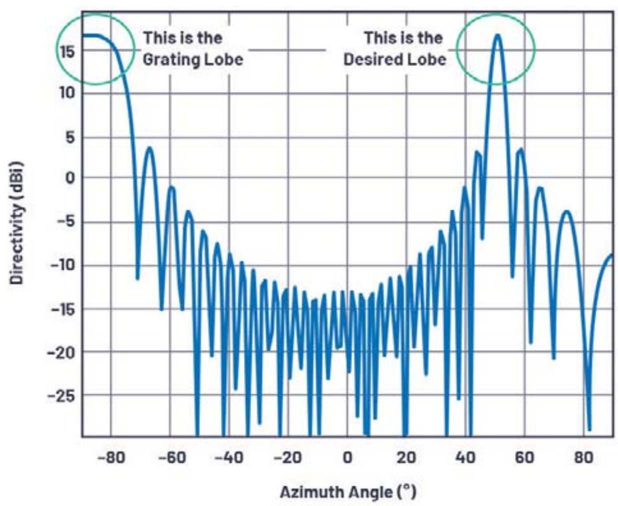

4. Grating lobes begin to appear at the horizon for θ = 50°, N = 32, d = 17 mm, and Φ = 10 GHz.

reduced scan angle (θmax), where θmax is less than π/2 (90°). For example, if the signal frequency is 10 GHz and we need to steer ±50° without grating lobes, then, as *Figure 4* shows, the maximum element spacing is:

$$d_{max} = \frac{(3 \times 10^8)/(10 \times 10^9)}{1 + \sin(50°)} = 17 \text{ mm} \qquad (13)$$

Thus, restricting the maximum scan angle brings a freedom to extend the element spacing to increase the physical size per channel as well as extend the aperture for a given number of elements. An example application that could exploit this phenomenon is for an antenna assigned to a narrow, predefined direction. The element gain can be increased for directivity in the predefined direction; the element spacing also can be increased for a larger aperture. Both result in larger overall antenna gain within the narrowed beam angle.

Note that Equation 3 indicates a maximum spacing of one wavelength, even for zero steering angle. This is the case if grating lobes can't be tolerated in the visible hemisphere. In the case of a GEO satellite, for example, the entire Earth is covered with a steering angle of 9° from mechanical boresight. It may be the case that grating lobes can be tolerated, if they don't land on the Earth's surface. In such a case, the element spacing may be several wavelengths, resulting in even more narrow beamwidths.

Also worth noting are antenna architectures that attempt to overcome the grating-lobe problem by producing a non-uniform element spacing. These are categorized as aperiodic arrays, with spiral arrays as an example. For mechanical antenna construction reasons, it may be desirable to have a common building block that can be scaled to a larger array, but this would produce a uniform array that's subject to the grating-lobe conditions described. **mw**

PETER DELOS is Technical Lead and **BOB BROUGHTON** is Director of Engineering for Analog Devices' Aerospace and Defense Group; **JON KRAFT** is Senior Staff Field Applications Engineer at Analog Devices.

REFERENCES

Balanis, Constantine A. Antenna Theory: Analysis and Design, third edition. Wiley-Interscience, 2005.

Longbrake, Matthew. True Time Delay Beamsteering for Radar. 2012 IEEE National Aerospace and Electronics Conference (NAECON), IEEE, 2012.

Mailloux, Robert J. Phased Array Antenna Handbook, second edition. Artech House, 2005.

O'Donnell, Robert M. "Radar Systems Engineering: Introduction." IEEE, June 2012.

Skolnik, Merrill. Radar Handbook, third edition. McGraw Hill, 2008.

New Products

Bias Tee Energizes 1.5 to 28.5 GHz

Mini-Circuits' model MBT-283 is a 50-Ω MMIC bias tee with high RF-to-dc isolation and low insertion loss from 1.5 to 28.5 GHz. Supplied in a surface-mount-technology (SMT) MCLP housing measuring 3.5 × 2.5 mm with 16-lead contacts, the RoHS-compliant bias tee is a good fit for match biasing amplifiers and laser diodes. It features typical isolation of 47 dB, typical insertion loss of 0.7 dB, and 20-dB typical return loss across the full frequency range. It can handle as much as 1 W (+30 dBm) of RF power and as much as 500 mA of dc current at +35 V dc.

MINI-CIRCUITS, https://www.minicircuits.com/WebStore/dashboard.html?model=MBT-283%2B

SP6T Switch Matrix Channels DC to 50 GHz

Mini-Circuits' model RC-1SP6T-50 is an electromechanical single-pole, six-throw (SP6T) switch matrix with wide bandwidth of dc to 50 GHz. Well suited for automated-test-equipment (ATE) and system applications, the RoHS-compliant switch features a break-before-make configuration to prevent accidental connections. The switch, controllable by USB or Ethernet interface, maintains low insertion loss across a wide frequency range, typically 0.2 dB from dc to 18 GHz, 0.3 dB from 18 to 40 GHz, and 0.4 dB from 40 to 50 GHz. Isolation between ports is typically 60 dB from dc to 18 GHz and 50 dB or more from 18 to 50 GHz. The switch is well matched to 50 Ω, with typical VSWR of 1.20:1 from dc to 18 GHz, 1.30:1 from 18.0 to 26.5 GHz, and 1.60:1 from 26.5 to 50.0 GHz. The SP6T switch matrix measures 6.00 × 5.50 × 2.75 in. (152.40 × 139.70 × 69.85 mm) with female 2.4-mm RF connectors. It is designed for typical cold switching power of 20 W to 18.0 GHz, 10 W to 26.5 GHz, and 3 W to 50 GHz and built for high reliability, rated for 2 million typical switching cycles.

MINI-CIRCUITS, https://www.minicircuits.com/WebStore/dashboard.html?model=RC-1SP6T-50

Spectrum Analyzers Feature VNA Measurement Mode

RIGOL Technologies' new RSA3000N and RSA5000N spectrum analyzers extend the flexibility and capability of the company's UltraReal platform with a new vector-network-analyzer (VNA) measurement mode. The instruments deliver the same performance specifications and feature set as the current RSA models but add the VNA capability as a standard feature. With integrated Smith charts, polar charts, reflection coefficient, impedance, insertion loss, frequency response, and a host of other measurements, the RIGOL UltraReal Spectrum Analyzer becomes a fully functional VNA. Supporting S_{11}, S_{21}, and distance-to-fault analysis, the RSA5000N and RSA3000N provide a valuable resource to engineers needing to tune antenna sets, search for communication and cable faults, or fully characterize their active or passive RF components. Prices start at $2,299 for a 1.5-GHz RSA3000N and at $8,999 for a 6.5-GHz RSA5000N model.

RIGOL TECHNOLOGIES, www.rigolna.com

Edge-Computing Platform Integrates CPU, Storage, and Networking

ADLINK Technology recently announced its collaboration with Intel to produce the MECS-6110 edge-computing system for Universal Customer Premise Equipment (uCPE). This general-purpose platform integrates compute, storage, and networking on a server. The MECS-6110 is outfitted with a single Intel Xeon D-2100 14-core processor, four DDR4 RAM slots, two SATA drive bays, and three M.2 slots. It also features a pair of PCIe x16 Gen 3 FHFL expansion slots and provides all I/O connection options on the front of the rack for easy access.

ADLINK TECHNOLOGY, www.adlinktech.com

COM Express Module Puts Server-Level Performance in the Field

Eurotech recently launched its CPU-162-23, a COM Express Type 7 module, which is outfitted with Intel's Xeon/Pentium D-1500 processors and supports up to four DDR4 SO-DIMM modules with 64 GB of RAM. The module is designed for rugged and HPEC applications and comes equipped with a myriad of interfaces, including up to 32 PCIe lanes, and two 10-Gb/s and one 10/100/1000-Mb/s Ethernet ports. It also offers two SATA 3.0, four USB 3.0, and four USB 2.0 ports. Eurotech states the CPU-162-23 COM Express Type 7 Module is a reliable platform for industrial and transportation applications and is designed to deliver supercomputer processing and data-center networking to the edge.

EUROTECH, www.eurotech.com

System Tests RF-over-Fiber Links for EMC/EMP Sturdiness

PPM Test has released its Sentinel 3 test and measurement system for a myriad of applications, including EMC conformance, HIRF aircraft clearance, simulated lightning testing, and more. The system offers five Tx8 transmitters and a chassis Rx6 receiver, which can accept up to six single or dual receiver modules. The platform features three modes: a low-noise mode, a high-power mode, and a high-impedance mode with increased sensitivity; lower test field strength; and reduced ERP. The Sentinel 3 comes outfitted with a touchscreen with a system controller that provides remote gain control, remote power up/down of transmitters, automatic unit detection, self-test, and more.

PPM TEST, www.ppmtest.com/products

This index is provided as an additional service by the publisher, who assumes no responsibility for errors or omissions.

Subscription Assistance and Information: (ISSN 0745-2993)

Microwaves & RF is published monthly. Microwaves & RF is sent free to individuals actively engaged in high-frequency electronics engineering. In addition, paid subscriptions are available. Subscription rates for U.S. are $95 for 1 year ($120 in Canada, $150 for International). Published by Endeavor Business Media, 1233 Janesville Ave., Fort Atkinson, WI 53538. Periodicals Postage Paid at Fort Atkinson, WI and additional mailing offices. POSTMASTER: Send change of address to Microwaves & RF, PO Box 3257, Northbrook, IL 60065-3257. For paid subscription information, please contact Microwaves & RF at PO Box 3257, Northbrook, IL 60065-3257. Canadian GST #R126431964.

Back issues of MicroWaves and Microwaves & RF are available on microfilm and can be purchased from National Archive Publishing Company (NAPC). For more information, call NAPC at 734-302-6500 or 800-420-NAPC (6272) x 6578.

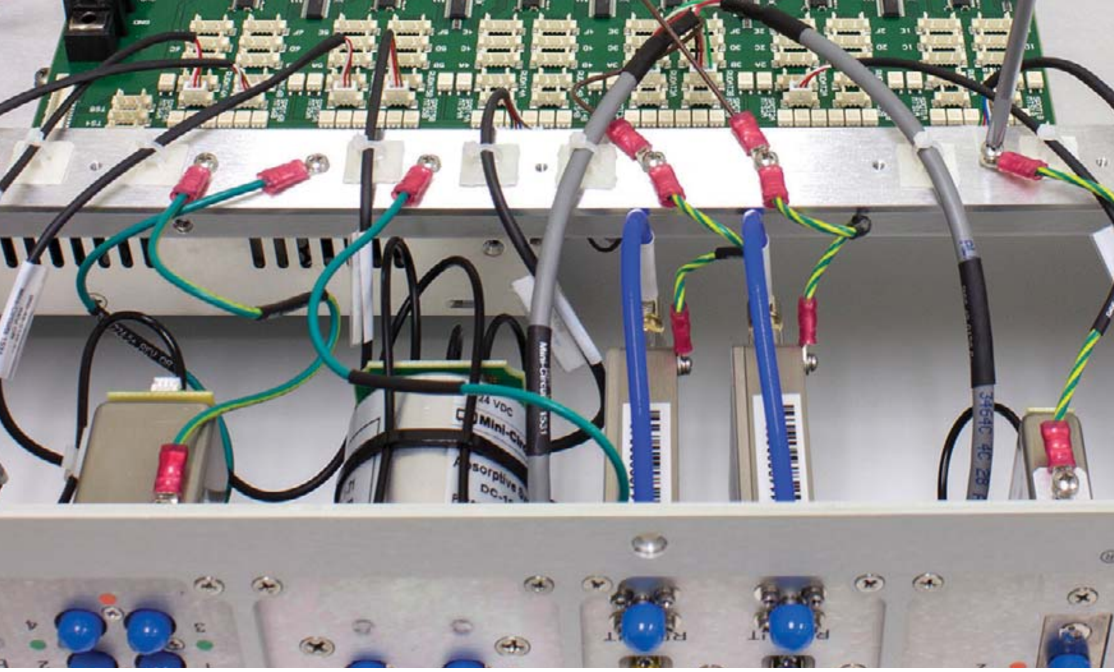

DC TO 50 GHZ

Test Solutions

Components, Systems and Accessories

User-Assembled

Leverage our wide selection of in stock components for total flexibility to build your own system. We'll help you choose the right hardware. You take it from there.

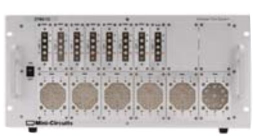

Pre-Built Modular

Configure our flexible, pre-built modular chassis structures with your choice of routing and attenuation hardware for delivery as fast as two weeks. Plug and play GUI and API included.

Custom Systems

Put our full design and manufacturing capability to work for you to build complex custom systems with bespoke control software tailored to your unique test setup—scalable from design to production.

Mini-Circuits®